SONIC LOGGING AT DYE-3, GREENLAND

by

KENDRICK C. TAYLOR, JR.

A thesis submitted in partial fulfillment of the requirements for the degree of

MASTER OF SCIENCE

(Geophysics)

at the

UNIVERSITY OF WISCONSIN-MADISON

1982

ABSTRACT

Sonic velocity logging of vertically traveling P-waves was performed at Dye-3, Greenland. Velocities range from 3745 m/s at a depth of 84 m to 3900 m/s at 1767 m, where an abrupt increase of 75 m/s is noted. This increase occurs at the Holocene-Wisconsin boundary. After the increase, the velocity averages 3975 m/s to the bottom of the ice sheet at 2037 m. The ice fabric can be modeled by an even distribution of c-axes in a vertically oriented cone. The "cone angle" (half the apex angle) ranges from 50° at 500 m to 20° below 1770 m. The ice fabric can be used to predict horizontal P-wave velocity which ranges from 3805 m/s at 700 m to 3820 m/s at 1750 m. The velocity profile at Byrd Station, Antarctica, is similar to the Dye-3 data. Agreement of measured vertical and predicted horizontal velocities with measurements made on the core are within the predicted errors.

A synthetic seismogram for a vertical reflection shows that reflections from within the ice sheet would have amplitudes 50 to 75 times smaller than the ice/rock reflection at the bottom of the ice sheet.

APPROVED: 

Charles R. Bentley
Professor of Geophysics
Major Advisor

ACKNOWLEDGEMENTS

I wish to acknowledge the help of Don Blankenship for enduring many "brain storming" sessions, and Ben Abernathy and Lee Powell for construction of and advice on the new uphole electronics.

Alison N. Mares typed the thesis; Susan H. Smith assisted with drafting.

Special thanks go to Dr. Charles R. Bentley, my Major Advisor, for making this work possible.

This work was supported by National Science Foundation grant DPP82-5614.

TABLE OF CONTENTS

LIST OF FIGURES

LIST OF TABLES

1. INTRODUCTION

The Greenland Ice Sheet Program (GISP) was an international interdisciplinary program to determine the geophysical and geochemical properties of the Greenland Ice Sheet. The primary goal was recovery and examination of an ice core to bedrock. The University of Copenhagen drilled at Dye-3 (65°11'N, 43°50'W) during the summers of 1979, 1980, and 1981. The core provides information on the structure and composition of the ice sheet.

The University of Wisconsin conducted sonic logging of the hole during 1982. The resulting velocity profile can be used to study the vertical variation of the ice fabric. In this paper the P-wave velocity data are presented and interpreted with respect to the crystal fabric. Predicted horizontal P-wave velocities and synthetic seismograms of a vertically traveling wave are also presented, as is a comparison to the analysis of the core.

2. INSTRUMENTATION

2.1 BACKGROUND

The instrumentation for this survey is based on a logger designed and built in 1969 by the Simplex Corporation of Dallas, Texas. The unit was designed for operation in ice sheets and only one has been built.

The borehole unit (BHU) contains a transmitter and four receivers which are suspended below the transmitter. When the transmitter fires it sends a sync pulse to the surface electronics which measure the difference in the arrival time of the wave front between two of the receivers. Given this time and the receiver separation, the velocity of the propagating wave is easily calculated. Figure 1 shows the BHU and the travel path of a wave refracting through the ice.

The original surface electronics contained an automatic zero crossing detector and chart recorder to display velocity in real time. This unit was perhaps best noted for its history of failures and noise problems. Since it would have required extensive repairs, a completely new surface unit was built.

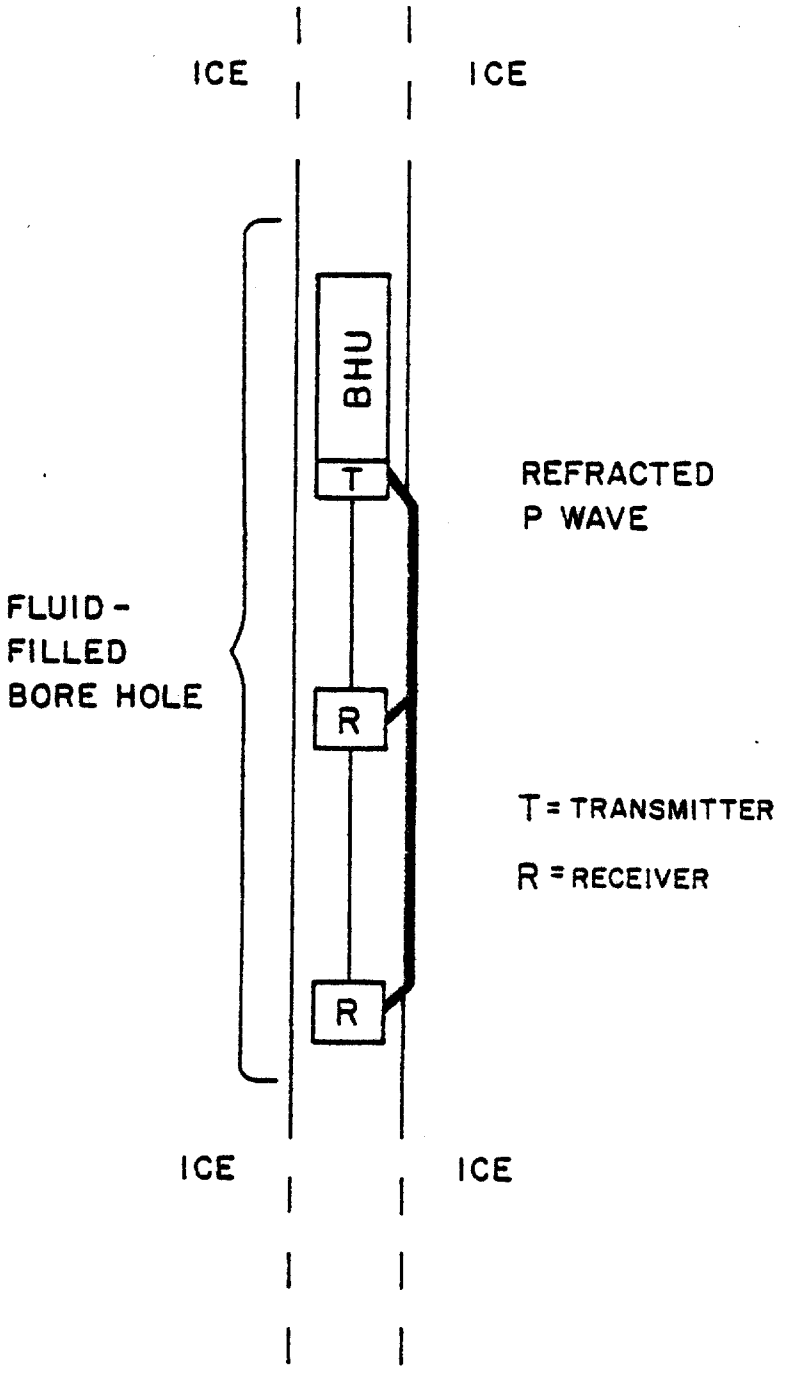

Figure 1. Borehole Unit

2.2 BOREHOLE UNIT (BHU)

The BHU remained essentially unchanged from its original design. The transmitter transducer with a peak frequency of 22 kHz fires 10 times per second and sends a sync signal up the cable. The BHU also alternately amplifies the signal from one of the two receivers. By alternating receivers, both receivers can use the same line in the cable to connect with the surface. On the surface the sync signal is then used to demultiplex the information from the two receivers. The transmitter unit contains all the down-hole electronics and is centralized by a bow spring system.

The receiver portion of the BHU consists of a cable with four crystal transducer receivers attached along it. In the original design the transducers were isolated from the borehole fluid by silicon oil and a rubber membrane. This is commonly done to prevent electrical contact between the borehole fluid and the transducers. The borehole at Dye-3 was filled with a non-conducting mixture of diesel fluid and perchloroethylene. Because it was not essential to use the silicone, oil and in view of the difficulties in filling the string with the oil, the transducers were operated with an open fluid connection to the borehole fluid. This was true for both the receiving and transmitting transducers. The receivers were centralized in the hole by a set of silicone rubber (RTV 630) fingers. The centralizers were no longer available commercially and were made in the lab.

There are two strings of receivers allowing a choice of receiver separations ranging from 0.67 m to 8.0 m. The shortest possible transmitter-to-receiver spacing is 1.4 m.

2.3 SURFACE ELECTRONICS

The need to design a new surface unit became apparent when it was realized this would be easier than repairing the 14-year-old surface set. To maintain timing, amplitude, and waveform information the new concept called for recording the received waveforms on a Honeywell Visicorder oscillograph. This configuration was an improvement over the old surface electronics which recorded only the time between two automatically-tracked zero-crossings. The need for timing errors of less than 2 μs was also noted.

To record the received signals on the visicorder it was necessary to have a delayed trigger and a pre-amplifier. Since the signals from both receivers were coming up the same line, two different delays and amplifications were required. It was also necessary to incorporate analog demultiplexing. Figure 2 shows a block diagram of the circuit. As the sync signal comes in it goes into a flip-flop which turns on the amplifier and delay circuits alternately for the near and far receivers. After the sync is delayed by the time set in the delay, it triggers the Visicorder. The Visicorder sweeps and displays the amplified signal. The next sync pulse, which corresponds to the other

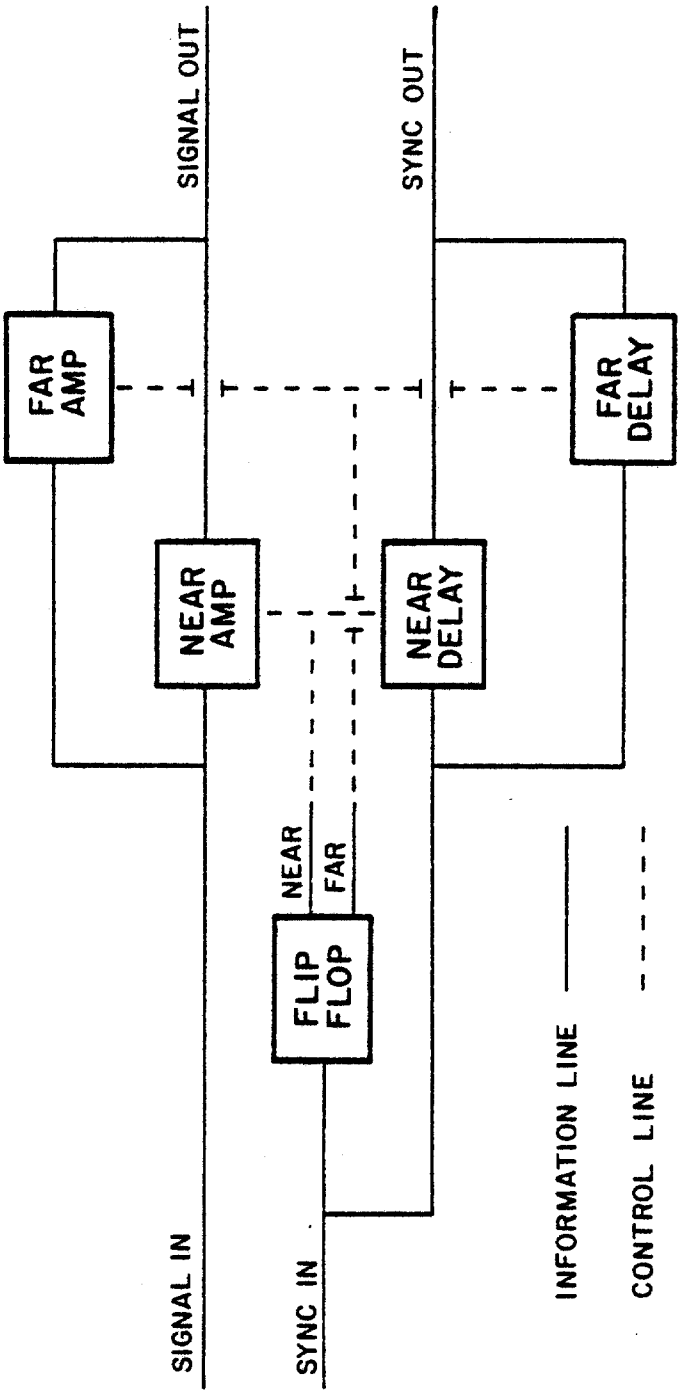

Figure 2. Surface Electronics

receiver, is routed by the flip-flop through the second delay, and then triggers the Visicorder which displays the signal from that receiver. The displays of the Visicorder are recorded on a roll of photographic paper. As the BHU is raised in the hole the Visicorder alternatively records the near and far waveforms on the roll of paper. The arrival time can be measured from the delay settings and Visicorder record. Because the waveform is recorded and the gain settings of the amplifiers are known, the amplitude information is also maintained. Figure 3 shows a sample record.

The digital delay counts cycles from a 1 MHz temperature-compensated crystal and is accurate to $\pm$ 1/2 μs, which is several times smaller than the uncertainty in picking the records. The unit has a restore button which generates a false sync pulse to correct for occasional noise bursts on the sync line which would otherwise cause the delays to be associated with the wrong signals. There is an output for a 100 kHz square wave for oscilloscope calibration. Appendix 1 contains a schematic, and a description of circuit operation.

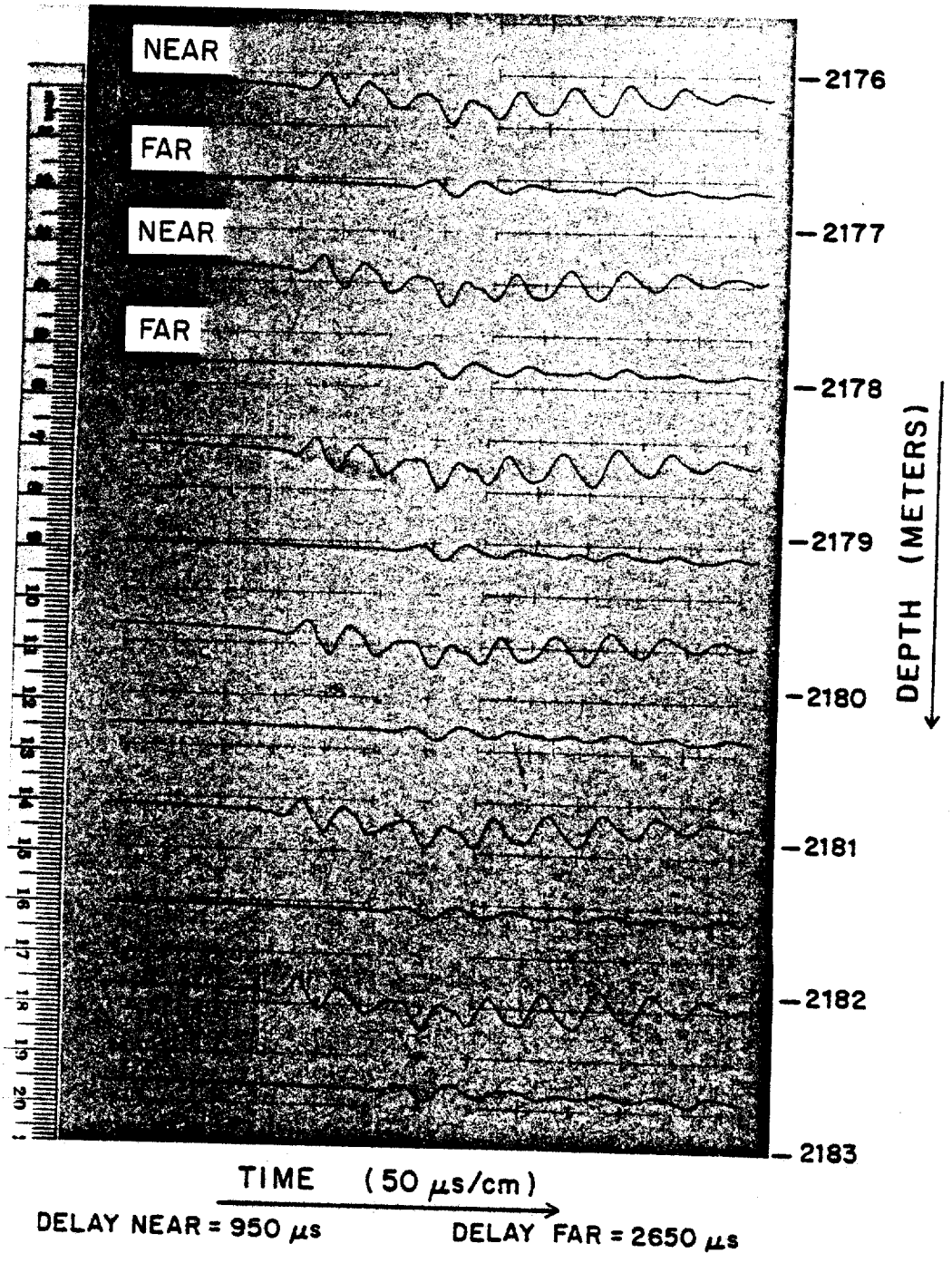

Figure 3. Sample Record

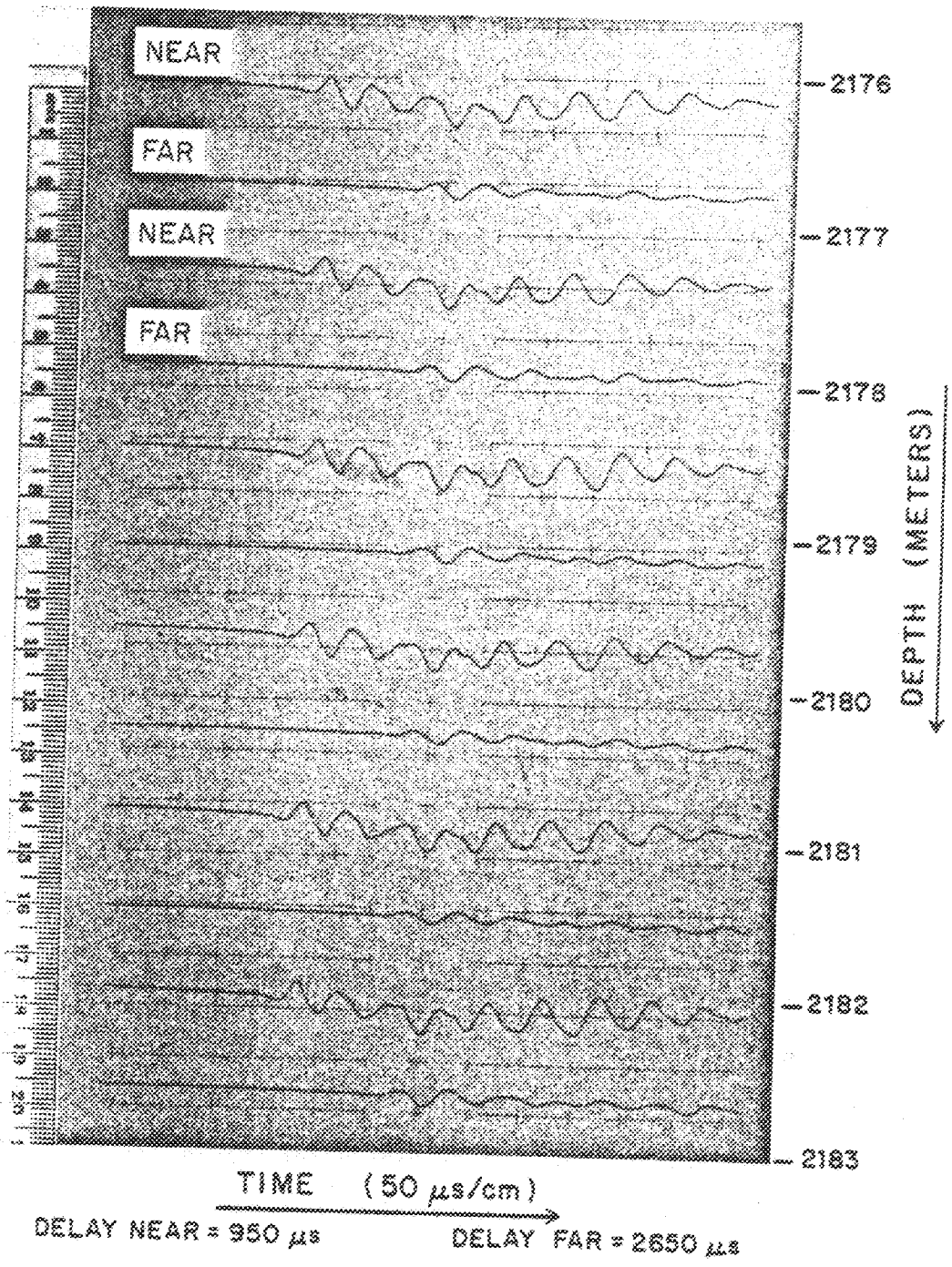

Figure 3. Sample Record

3. FIELD PROCEDURE

3.1 SET UP

The field program occurred during the first three weeks of July 1982. The winch was supplied by PICO (Polar Ice Coring Office) and had suffered water damage in shipment resulting in an inoperable hydraulic control valve. Water marks indicated that there had been 10 cm of water in the cab. The damage hampered the program because the damaged valve limited the pulling load at the winch to 1000 lb or about 10% of its rated maximum. As a result, we were only able to go to the bottom of the hole once and even that was risky as the winch could barely retrieve the cable.

There were also problems with the electrical grounding. Power was generated at the station about 1 km away and there was approximately a 70-volt potential difference between station ground and the top of the casing. Not only was this a problem for the equipment but also a hazardous situation as shocks were frequent. The problem was compounded by the design of the BHU, which uses the BHU housing and the cable armor as a ground return to the surface. Hence, as the BHU moves in the hole it encounters different ground potentials in the ice. At the same time, the cable can contact the casing which is possibly at another potential. All grounds were tied together which helped somewhat, but there was still 60-Hz noise on the ground lines.

Once the grounding problems were corrected, the flaws in the equipment were approachable. The new surface electronics had a jitter of approximately 10 μs in the delay. The source of this problem was two-fold: first, it was necessary to trigger on the front side of the sync pulse as this was more stable than the back side, and secondly, there were a few logic errors in the design. These problems were corrected in time. The floating grounds continued to be a problem and a capacitor was used to filter out frequencies below 200 Hz on the signal line.

3.2 TESTING

The first significant test was a record which showed the total wave train. Figure 4 was recorded at a depth of 150 m and shows the total wave form at both the near and the far receivers. The P-wave refracted through the ice and the fluid wave are both seen. The large-amplitude low-frequency signals on the far receiver are noise. They are believed to have their origins in RF coupling to the transmitter-charging circuit. The floating grounds may also have been partially responsible for this.

Shear waves or fluid/ice boundary waves traveling at shear velocities would be expected to arrive between 2100 m/s and 1700 m/s. No strong arrivals are seen. There are some weak arrivals but their low amplitude and emergend onset limit their usefulness. Preliminary results from Dome C, Antarctica, show shear arrivals within this same BHU and receiver spacing. Their

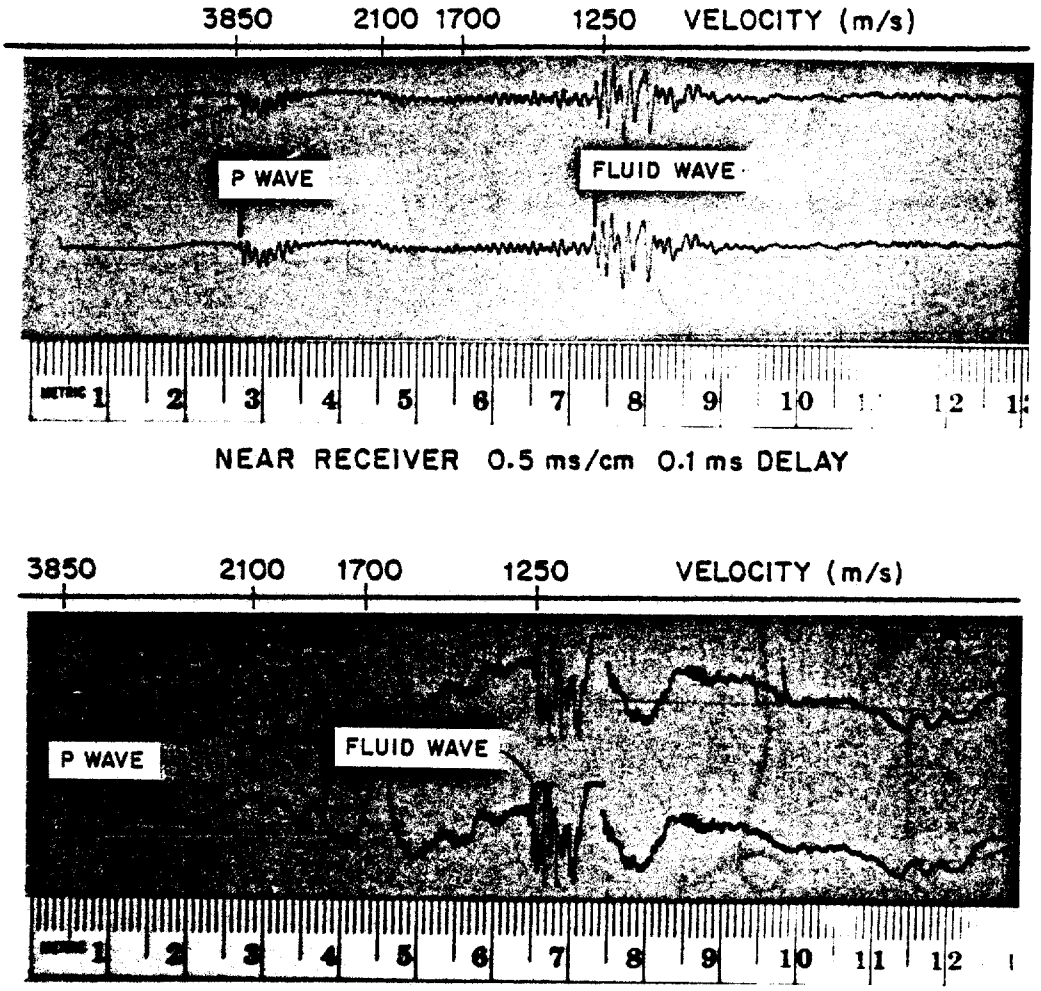

Figure 4. Total Wave Record

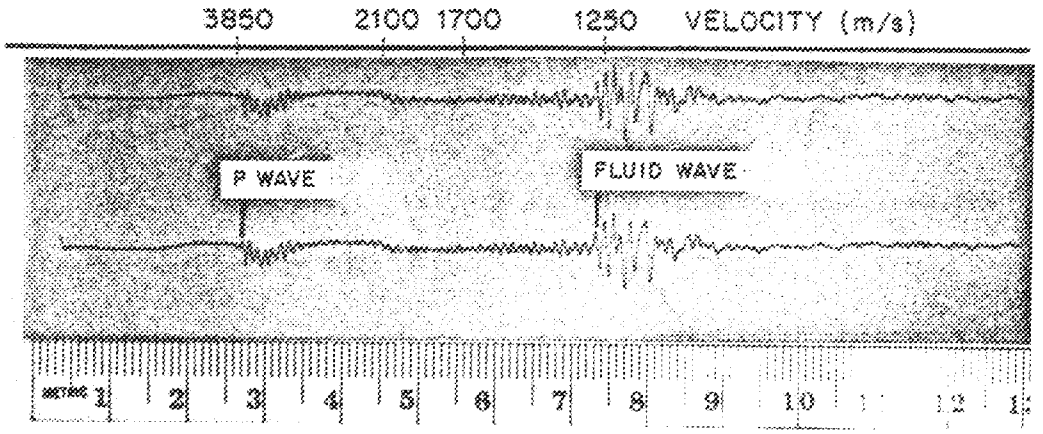

Figure 4. Total Wave Record

amplitude, however, is about half of the P-wave amplitude at the near receiver and one-fifth of the P-wave amplitude at the far receiver. Such low amplitudes would be only marginally present in the noisier Dye-3 data.

The next important test was to prove that the measurements were repeatable and consistent with other methods. As a check on timing accuracy, the travel time difference for the first peak of the P-wave was measured by both the new surface electronics and a HP 175A scope. The scope was first calibrated by comparison of its delay trigger with a 100 kHz signal provided by the crystal oscillator in the surface electronics. The error in the delay circuit of the oscilloscope, which was non-linear and temperature-dependent, was used to correct the oscilloscope readings. A comparison of the time as measured by the oscilloscope and surface electronics/visicorder system are shown in Table 1. Since the clock pulse is 1 μs, accuracy greater than that should not be expected. The average error of 0.5 μs shows that the surface electronics were not introducing any unknown delays. Because the oscilloscope was calibrated to the same time base, this does not prove that the times were correct in an absolute sense, just that the digital delay was working as designed. The clock oscillator was checked before departure and was within its error specifications of less than one part in 10^{-7}.

TABLE 1

Accuracy of Travel Time Measurements

Date	Depth (m)	Travel Time HP 175A (μs)	Travel Time Surface Electronics (μs)	ΔT (μs)
July 8	165	1819.5	1820.5	1.0
July 12	165	1821.5	1821.5	0.0
July 12	295	1816.5	1817.0	0.5

The other important test was to show that the measurements are repeatable. To do this, the BHU was stopped at selected depths on the way down the hole and a record was taken. This travel time was compared to the time as measured on the continuous run on the way up the hole. The time difference between the two sets of measurements varied from 30 minutes at the bottom of the hole to several hours at the top. The results are tabulated in Table 2 and show an average error of 0.04 μs with a maximum of 2.0 μs. This is well within the expected range.

3.3 DATA ACQUISITION

The hole was logged in three separate continuous runs with a receiver spacing of 6.993 m. It was occasionally necessary to stop the winch due to hydraulic problems for a few minutes at a time. After stopping, the BHU was lowered at least 20 m and brought back to provide some overlap. Consecutive runs overlap by at least 10 m. At its deepest, the bottom of the logger was 23 m from the bottom of the hole. Cable length was measured by a wheel of known circumference and was marked on the records every 50 feet. Unfortunately, due to the poor performance of the winch hydraulics it was not possible to make any more runs.

TABLE 2

Repeatability of Travel Time Measurements

Depth (m)	Travel Time @ T_1 (μs)	Travel Time @ T_2 (μs)	ΔT μs
590	1814.0	1815.0	1.0
689	1810.0	1810.0	0.0
787	1810.5	1810.0	-0.5
886	1809.0	1810.0	1.0
985	1801.0	1802.0	1.0
1083	1800.0	1800.0	0.0
1181	1793.0	1795.0	2.0
1281	1786.0	1784.5	-1.5
1378	1780.0	1781.0	1.0
1476	1777.5	1776.0	-1.5
1571	1740.0	1740.0	0.0
1674	1788.0	1786.0	-2.0
1771	1793.0	1792.0	-1.0
1864	1797.0	1797.0	0.0

4. DATA REDUCTION

4.1 DEPTH DETERMINATION

All depth measurements mentioned so far express the distance of the top of the BHU below the top of casing extension that PICO added in late June 1982. To reduce this depth reading to a datum based on the top of the casing during drilling, it was necessary to subtract the height of the new casing, 12.79 m. To assign the measured velocity to a depth corresponding to the center of the receivers, it is necessary to add 9.93 m. It is also necessary to consider stretch in the cable. Appendix 2 explains this calculation which shows the elongation of the cable at the bottom to be less than 2.0 m.

All further depth measurements are corrected for the casing height, logger length and cable stretch.

4.2 AMPLITUDE AND WAVEFORM ANALYSIS

One of the advantages of the new surface electronics is that it provides a permanent record of the received signals. This is useful for checking the quality of the data. In boreholes that have an irregular shape, the travel times will be effected by odd travel paths if the BHU is not centered or if there is a cavity in the vicinity of one of the receivers. These odd travel paths will cause amplitude variations in the received signal.

The new surface unit maintains amplitude and waveform information. The records show no measurable changes with depth in amplitude or waveform of the first P-wave peak. Variations most likely due to arrivals from multiple paths were noted in later cycles. For an amplitude variation to be detectable there would have to be a change of at least 3 dB. It is important to note that this hole was electromechanically drilled, which resulted in an exceptionally smooth borehole varying from 130.0 mm in diameter at the top to 129.5 mm at the bottom. The consistency of the bore diameter resulted in very high quality P-wave data.

4.3 VELOCITY DETERMINATION

The major job in reducing the data was picking the arrivals. The paper records were picked every 3.33 m of borehole length, which is slightly less than half of the receiver separation. At each sample depth the three closest first peaks were picked and a line was drawn through them. The distance between the line for the near and far receiver was then measured to $\pm$ 0.1 mm, which corresponds to 1.0 µs. The measurements were repeatable to 2.0 µs. This averaging of three traces resulted in an averaging of the velocity over a 0.5 to 1.5 m range, depending on the winch speed. Where runs overlapped, differences were less than 2.0 µs and the average was taken. Velocities were calculated by dividing the distance between the receivers by the travel time between them, 6.993 m.

4.4 ERRORS

Errors in depth of measurement could be the result of a delay in marking the depth on the moving paper record and errors in the calculation of the cable stretch. The combined total is believed to be less than 3 m. Errors in relative velocity come mainly from picking errors. The top of the peaks that were picked could be defined to about 0.4 mm, which corresponds to 2.0 μs. This is a limitation of the frequency of the BHU transmitter. Another possible source of timing errors is nonlinearity in the sweep rate of the Visicorder. Calibrations showed the center portion of the sweep was linear with respect to time, and correctly calibrated at 50 μs/cm. The digital delays were set to keep the arrivals close together and in this portion of the record, so no Visicorder corrections were necessary. The uncertainty of 2 μs corresponds to approximately a 5 m/s uncertainty in the final relative velocities.

Errors in absolute velocity may be caused by using an incorrect distance for receiver separation or the clock crystal being off-frequency. The temperature compensated crystal was checked prior to leaving and was within its specifications; errors due to it would be negligible. The measured receiver separation of 6.993 m was measured with the receiver string hanging in air, rather than fluid as in the borehole. There is also some uncertainty as to the location of the receiver crystals in

the receiver housings. These problems lead to an uncertainty of 2.0 cm in the receiver separation, or an error in absolute velocity of 10 m/s.

As explained in Section 5.2.3, the difference between the vertical velocity and the velocity measured parallel to the borehole is about 4.5 m/s at 1500 m and 7 m/s at 1800 m.

5. DATA ANALYSIS

5.1 VELOCITIES

The curve of P-wave velocity vs. depth (Figure 5) has many notable features. The measurements start at 84 m with a velocity of 3745 m/s, which increases to 3842 m/s at 150 m. This rapid change is due to densification of the firn.

From 200 m to 1400 m, the velocity slowly increases to 3940 m/s. The uncertainty in relative velocity of 5 m/s is clearly seen as small rapid fluctuations in this section. From 1400 m to 1750 m the velocity decreases to 3900 m/s.

At 1767 m a rapid jump marks the Holocene-Wisconsin boundary. This jump of 75 m/s appears over a 7-m interval, but since the logger measures the average velocity over 7 m, the boundary could be much more abrupt. From 1775 m to 2008 m the velocity is approximately 3975 m/s.

There are several smaller variations, 15-40 m/s in amplitude, which are approximately 30 m thick. These variations, which occur at 1450, 1680, 1730, and 1920 m are believed to be real. The most likely explanation for them is a change in ice fabric.

Surface radar has been used to map the bedrock topography in the Dye-3 area (Jezek, personal communication, 1982). The local region is characterized by hilly terrain with elevation differences of hundreds of meters. There is an abrupt change in the

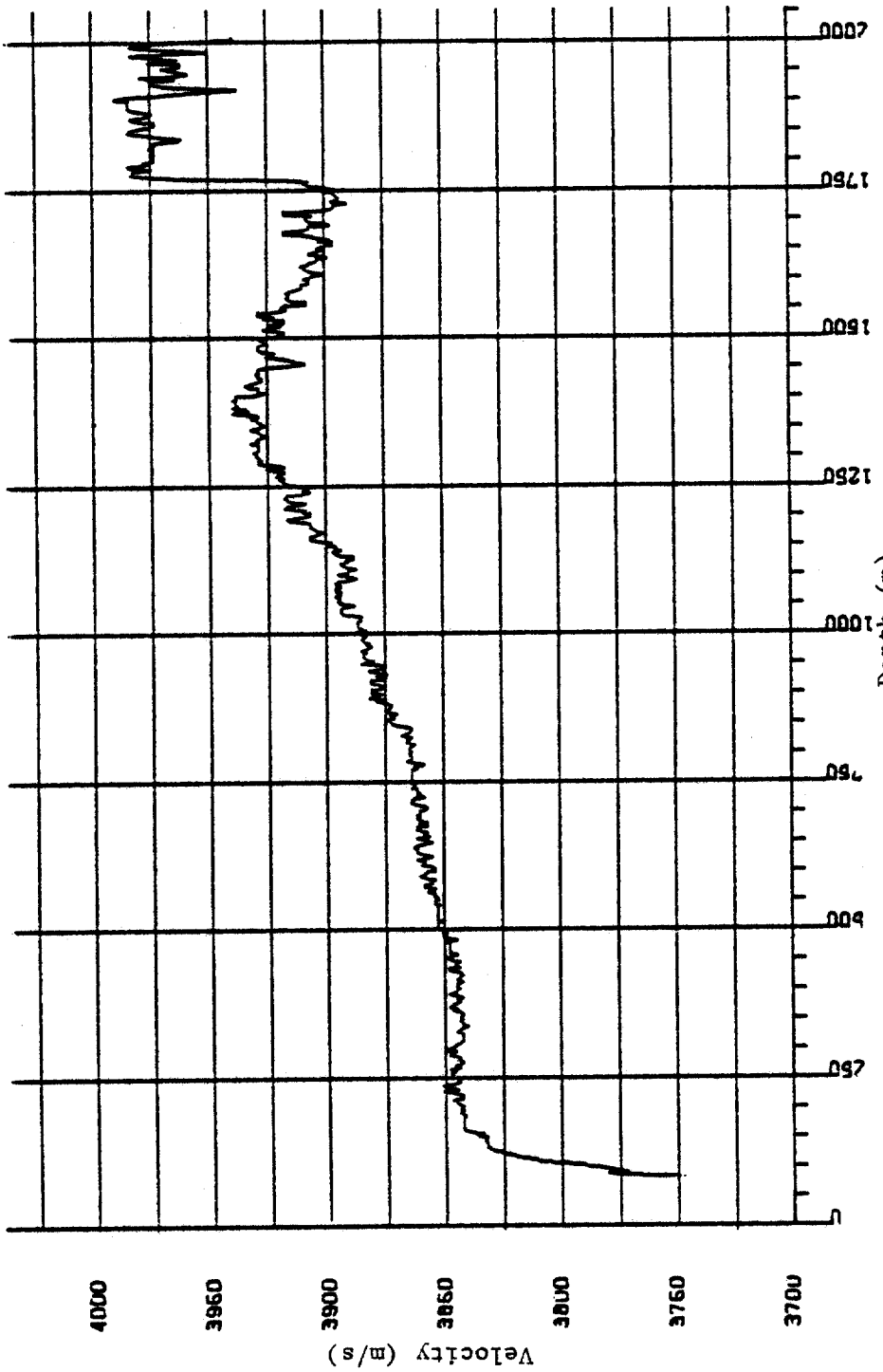

Figure 5. P Wave Velocity vs. Depth

character of the velocity curve 150 m above the bottom. The change is characterized by a sharp downward spike of 50 m/s and is followed by a zone of more rapid oscillations than are noted elsewhere. It is possible that this discontinuity of the lower 150 m marks a basal zone of deformed ice. This is supported by Dansgaard (1982) who reports a layer of bedrock origin at 87 m above the bottom. This layer is not noted on the velocity profile which averages over a 7 m interval.

Appendix 3 contains a tabulation of the velocity vs. depth relation.

Figure 6 shows the same velocity data corrected to a temperature of -10°C. The temperature profile, which was provided in advance of publication by Gundestrup (personal communication, 1982), is in Appendix 4. The value of -2.3 m/s°C, given by Kohnen (1974), was used to make the correction. The broad velocity high at 1400 m is still present but somewhat diminished in amplitude.

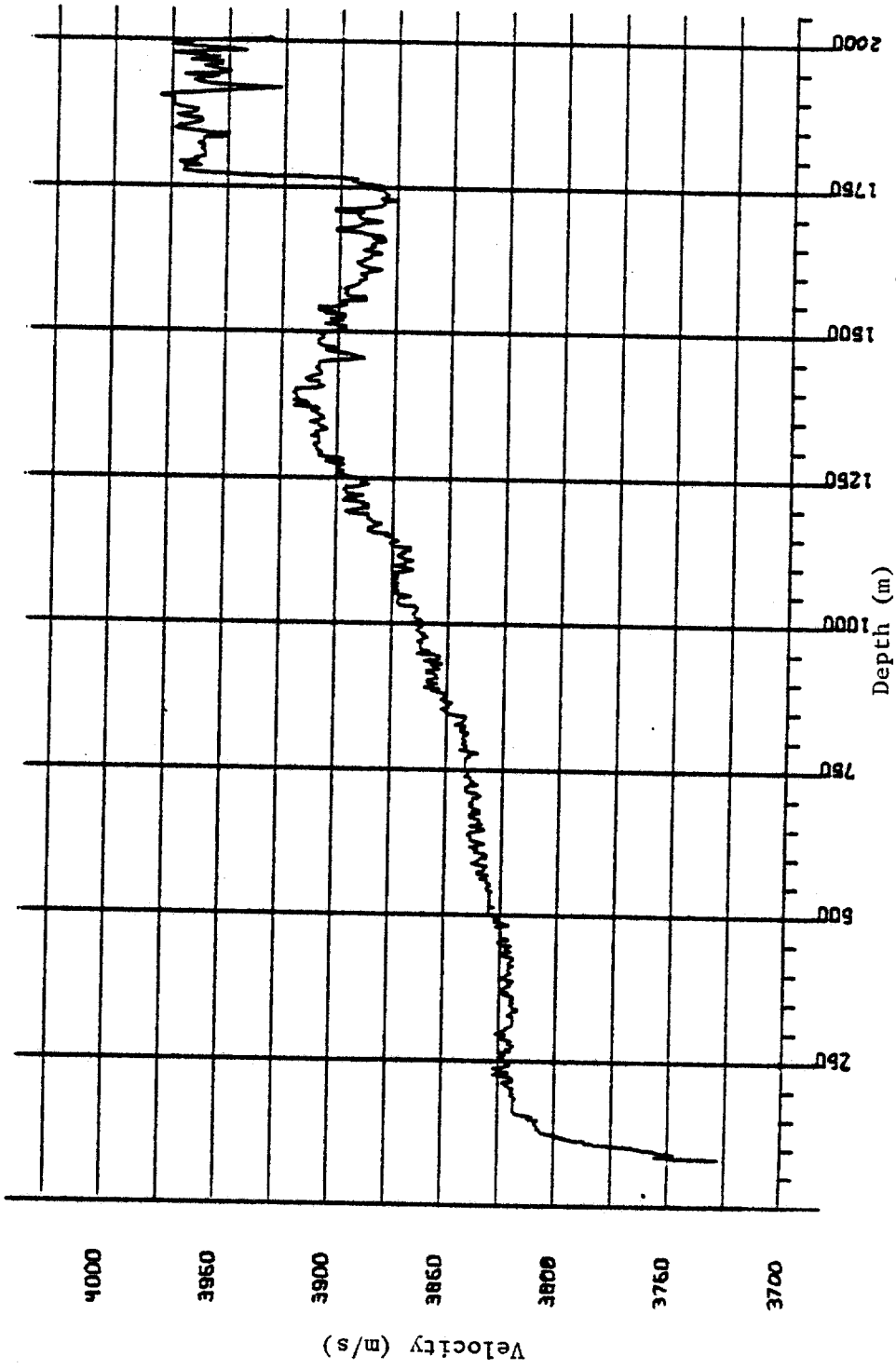

Figure 6. P Wave Velocity vs. Depth (at -10°C)

5.2 ESTIMATION OF CRYSTAL FABRIC

5.2.1 Background

The major influence on P-wave velocity in a single crystal of ice is the orientation of the crystal with respect to the direction of wave propagation. Bennett (1972) has derived this relation and, using elastic constants determined by himself and others, calculated the velocity as a function of the angle of propagation with respect to the crystal c-axis. Bennett (1968) also derived the velocity relationship for P waves and S waves in a crystal aggregate with a distribution of preferred crystal orientations. His method was to average slowness surfaces within the aggregate.

Bentley (1972), using data from Byrd Station, Antarctica, compared logged sonic velocities to velocities calculated from the measured fabric using Bennett's relationship. His results showed a difference between the two velocities at depths greater than 1200 m. He attributed this difference to the scatter resulting from fabric determinations in thin sections vs. logger measurements which are averaged over 20 m.

5.2.2 Procedure

Bennett's (1972) equation for P-wave velocity in a crystal aggregate uses a conical shape to describe the c-axis distribution. In his work he considers the two cases of the axis evenly distributed in the cone, and the axis distributed only on the cone's surface. The relationship includes the cone angle, I (the angle between the axis and side of the cone), and the propagation angle, σ (the angle between the cone axis and the direction of energy propagation). Equation 1 shows this relationship for a P-wave traveling in an ice aggregate with a solid cone distribution of c-axes.

$$V_p^{-1} = [255.16 + 37.2 \cos^2 I - 47.36 \cos^4 I + \sin^2 \sigma [5.92 (4-36 \cos^2 I + 40 \cos^4 I) - 5.08 (1-3 \cos^2 I)] - \sin^4 [5.92 (3-30 \cos^2 I + 35 \cos^4 I)] \times 10^{-6}] \quad (1)$$

Figure 7 shows Bennett's predicted P-wave velocity vs. the cone angle for propagation angles of 0 and 7°, which delimit the range of inclinations of the borehole.

Bennett's calculated value for isotropic ice at -10°C is 3871 m/s. This differs from Kohnen's (1974) value of 3818 m/s which was obtained by considering over 30 values obtained in Greenland and Antarctica. A correction of 53 m/s was also made to Bennett's values for this reason.

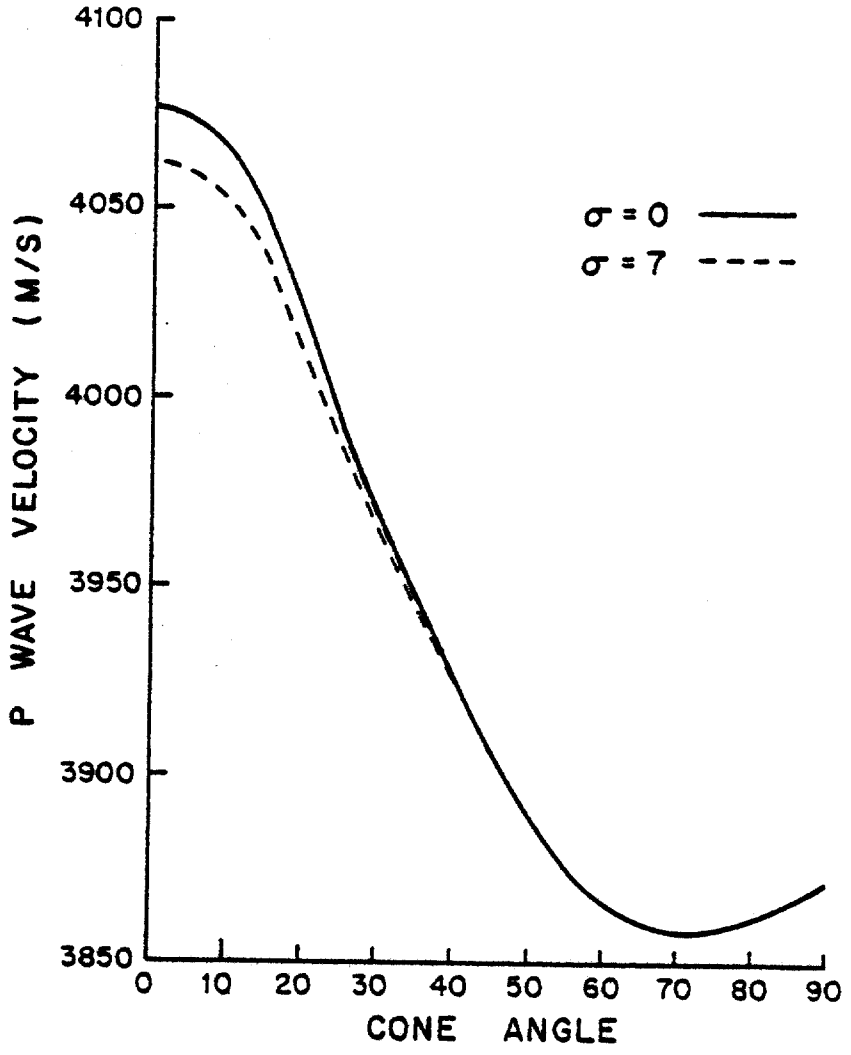

Figure 7. Predicted P-wave velocity vs. Cone angle

For the purpose of evaluating the crystal fabric, the cone orientation was assumed to be vertical, and the borehole inclination was used for the propagation angle. The inclination data were provided by Gundestrup (personal communication, 1982). Cone angles greater than 50° were not considered due to the low slope on the velocity vs. cone angle curve.

5.2.3 Results

Figure 8 is the predicted fabric. The cone angle first diminishes to 50° at a depth of 650 m; it decreases to 30° at 1400 m. The Holocene-Wisconsin boundary is seen at 1770 m as a rapid decrease in cone angle from 35° to 20°; the 20° angle is maintained to the bottom of the hole. The velocity events of 20 m/s in amplitude can be seen to require only a change of 5° in the cone angle.

Using this fabric interpretation it is possible to estimate the difference between vertical velocity and the measured velocity which is parallel to the borehole. The effects will be larger when the cone angle is small. Using Bennett's solid cone function the difference at 1500 m is 4.5 m/s and at 1800 m is 7 m/s, the vertical velocity being the faster.

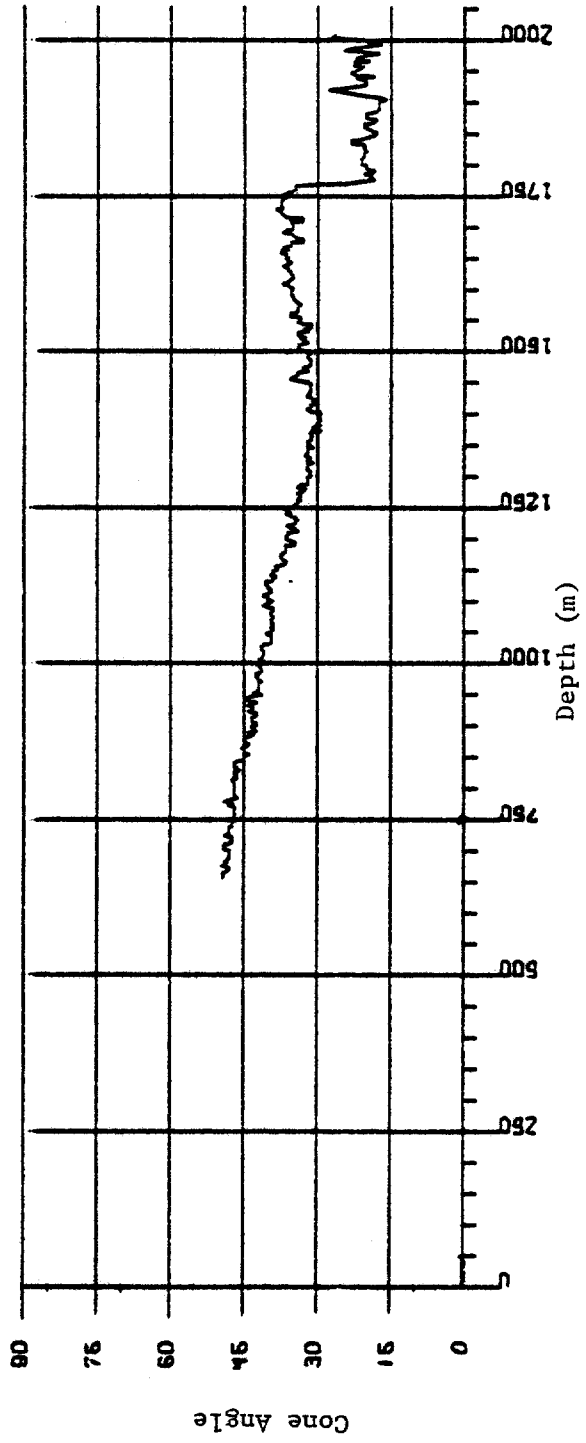

Figure 8. Calculated Cone Angle vs. Depth.

5.3 ESTIMATION OF P-WAVE VELOCITY PERPENDICULAR TO THE BOREHOLE

5.3.1 Procedure

The calculated fabric can be used to estimate the P-wave velocity perpendicular to the borehole. Setting σ in Equation 1 equal to 90 minus the borehole inclination angle yields the theoretical P-wave velocity perpendicular to the borehole. The theoretical P-wave velocity parallel to the borehole is found by setting σ equal to the borehole inclination. The difference of the theoretical parallel velocity and the theoretical perpendicular velocity (ΔV) can then be subtracted from the measured velocity values to obtain an estimate of the perpendicular P-wave velocity.

5.3.2 Results

Figure 9 shows the calculated perpendicular P-wave velocity at -10°C vs. depth. No values are given for depths less than 650 m because the fabric was not calculated above that depth. The velocity increases slowly from 3805 m/s at 700 m to 3820 m/s at 1750 m. The Holocene-Wisconsin boundary is marked by a jump to 3845 m/s.

If this were a simple two-layer case, a refraction survey could be considered to locate this boundary. However, with the existence of a zone at 1300 m in which the velocity is only about 15 m/s less than that in the Wisconsin ice, a more complicated model is required. Because of the small velocity contrast it

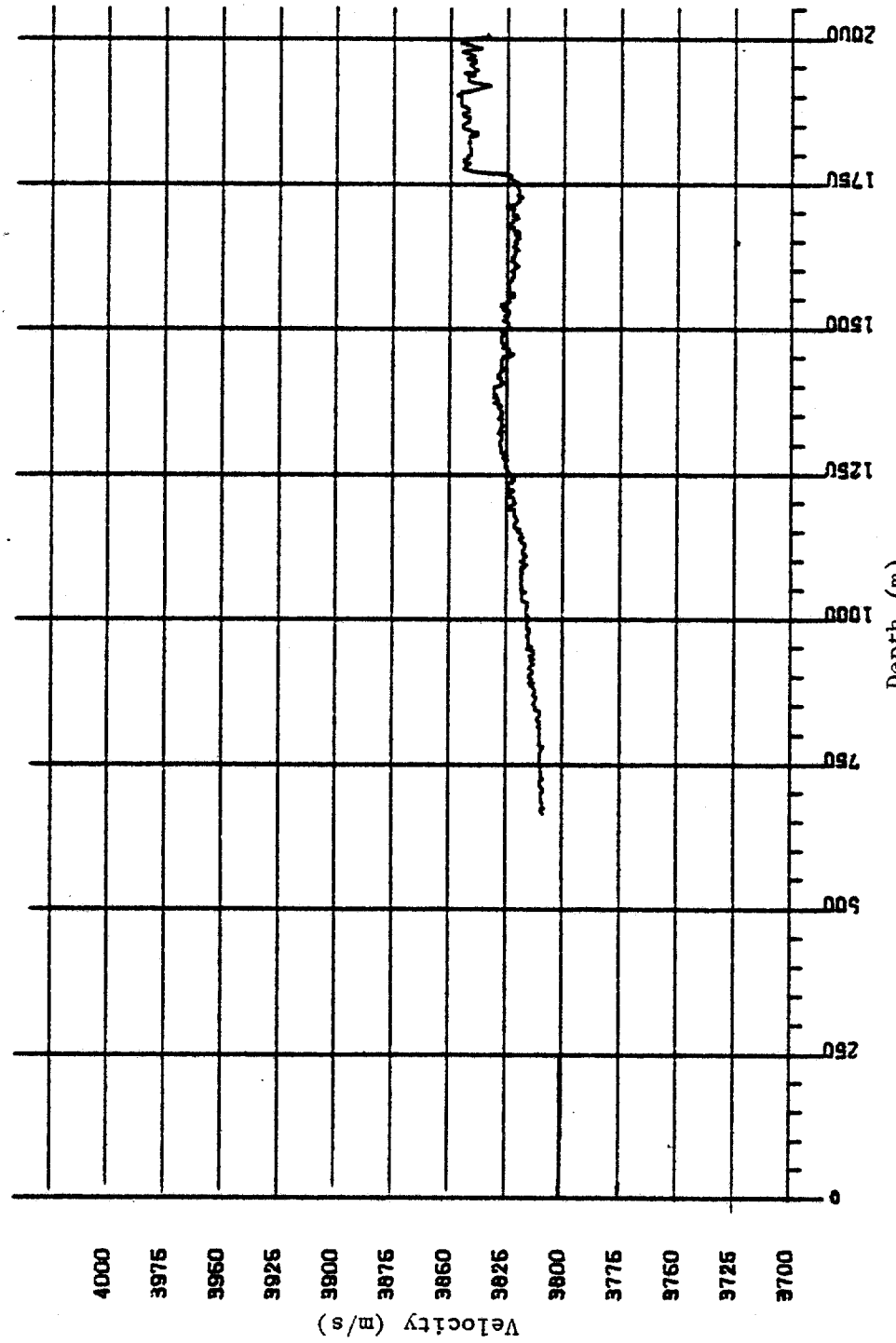

Figure 9. Predicted Perpendicular Velocity

would be difficult to decide on an appropriate model geometry beforehand.

5.4 SYNTHETIC SEISMOGRAM

5.4.1 Background

Given a velocity vs. depth and a density vs. depth profile it is possible to calculate what a vertical seismic reflection seismogram would be. Bentley (1971) noted the existence of pre-bedrock reflections in West Antarctica. Synthetic seismogram modeling can be used to investigate the possibility of similar reflections at Dye-3. The main advantage of calculating a synthetic seismogram over a simple comparison of the acoustical impedence ratios is that the synthetic seismogram takes into consideration the effect of closely-spaced reflections. In addition, it also yields the travel times.

5.4.2 Procedure

Figure 10 shows how the amplitude of a vertical traveling plane wave is effected by travel through two layers and reflection back through them. The incident wave passes the datum with an amplitude of 1; after traveling through the first layer it is attenuated by the amount A_1. Only a portion of the energy is transmitted across the boundary, so the amplitude is decreased by T_1 . The wave is further attenuated in layer 2 by A_2. If we consider the reflection at the bottom of layer 2 the reflection

DOWN TRAVELING	UPWARD TRAVELING	
(Incident Wave) 1.0	$A_1T_{1\uparrow}A_2R_2A_2T_{1\downarrow}A_1$	V_1,ρ_1,A_1,Z_1
	(reflection as seen at datum)	
A_1	$T_{1\uparrow}A_2R_2A_2T_{1\downarrow}A_1$	
$T_{1\downarrow}A_1$	$A_2R_2A_2T_{1\downarrow}A_1$	V_2,ρ_2,A_2,Z_2
$A_2T_{1\downarrow}A_1$	$R_2A_2T_{1\downarrow}A_1$ (reflection)	
$T_{2\downarrow}A_2T_{1\downarrow}A_1$		V_3,ρ_3,A_3,Z_3
(downward traveling wave)		

V_i = velocity, ρ_i = density, and Z_i = thickness in ith layer

$R_{1\downarrow}$ = Reflection coefficient for downward traveling wave at boundary 1-2 $= \dfrac{\rho_1V_1 - \rho_2V_2}{\rho_1V_1 + \rho_2V_2}$

$T_{1\downarrow}$ = Transmission coefficient for downward traveling wave at boundary 1-2 $= \dfrac{\rho_1}{\rho_2}\left[1 - R_{1\downarrow}^2\right]^{\frac{1}{2}}$

$R_{1\uparrow}$ = Reflection coefficient for upward traveling waves at boundary 1-2 $= \dfrac{\rho_2V_2 - \rho_1V_1}{\rho_1V_1 + \rho_2V_2}$

$T_{1\uparrow}$ = Transmission coeffient for upward traveling wave at boundary 1-2 $= \dfrac{\rho_1}{\rho_2}\left[1 - R_{1\uparrow}^2\right]^{\frac{1}{2}}$

A_1 = Attenuation and spreading loss $= \dfrac{1}{Z}\,c^{-\alpha Z}$

Figure 10. Synthetic Reflection Amplitude.

coefficient will be R_2. The upward traveling reflected wave will suffer similar attenuation and transmission losses as the downward traveling wave did. In the algorithm used to calculate the synthetic seismograms (Appendix 5), a separate layer was used for each measured velocity. This resulted in a model with over 600 layers.

By calculating the reflection amplitudes and converting the corresponding depths to time, a reflection amplitude time series is obtained. This time series can then be convolved with a wavelet to generate a synthetic seismogram.

The following assumptions were used in calculating the synthetic seismograms.

1. Time 0.0 occurs at 500 m;
2. A 100 Hz Ricker wavelet was used. Blankenship (personal communication, 1982) considers this to be a good simulation of the impulse from a surface shot;
3. The density of the bedrock is 2.70 gm/cm^3 (Jezek, personal communication, 1982);
4. The velocity in the bedrock is 5500 m/s;
5. The density of the ice is 0.917 gm/cm^3;
6. Attenuation in the ice is given by $e^{-\alpha x}$, $\alpha = .155\ km^{-1}$ (Bentley, 1977), and x is the distance traveled.

5.4.3 Results

In the first seismogram (Figure 11) the logged velocities values were used. In the bottom portion of the hole (2008 m to 2037 m), which was not logged, the velocity was assumed to be 3960 m/s,

The important aspect of this plot is the occurrence of small arrivals before the bottom reflection. Bentley (1971) noted the existence of pre-bedrock arrivals in West Antarctica, which he attributed to morainal debris in the ice. The ratio of the early arrival amplitude to the bedrock arrival amplitude was in the range of 0.07 - 0.26, with an average of 0.1. The amplitude ratio in the synthetic seismogram is 0.02.

A second seismogram (Figure 12) was calculated to investigate the maximum ratio for the reflection from an ice fabric boundary and an ice/rock boundary. The logged velocity values were used above 1900 m; below 1900 m the velocity was set at 3770 m/s to represent a bottom layer of isotropic ice. The amplitude ratio was 0.07. If the bedrock velocity were 2500 m/s, an exceptionally slow shale, for example, the amplitude ratio would double to 0.14. This unlikely, contrived, case would be an upper limit of the amplitude ratio. It could explain some, but not all, of the reflections noted by Bentley.

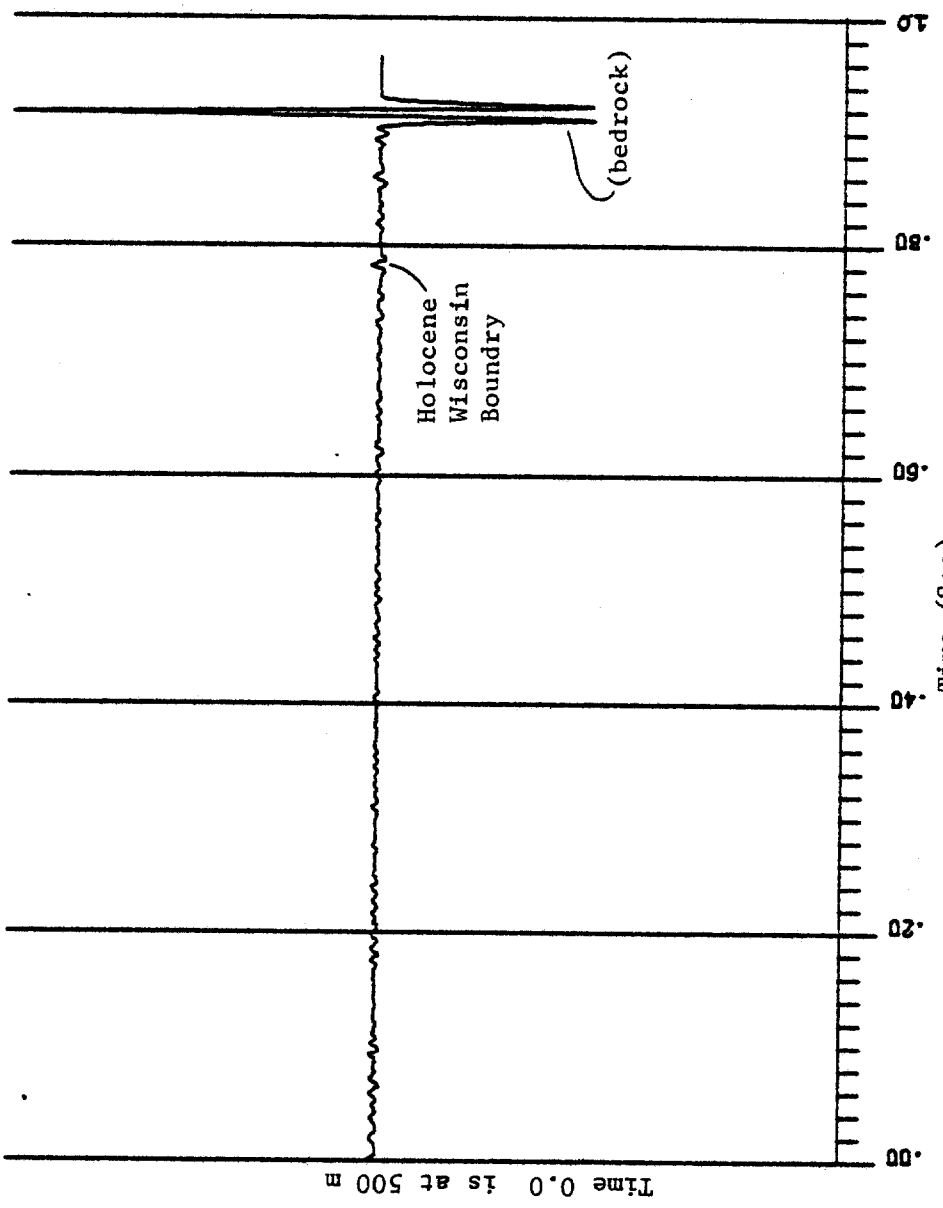

Figure 11. Synthetic Seismogram

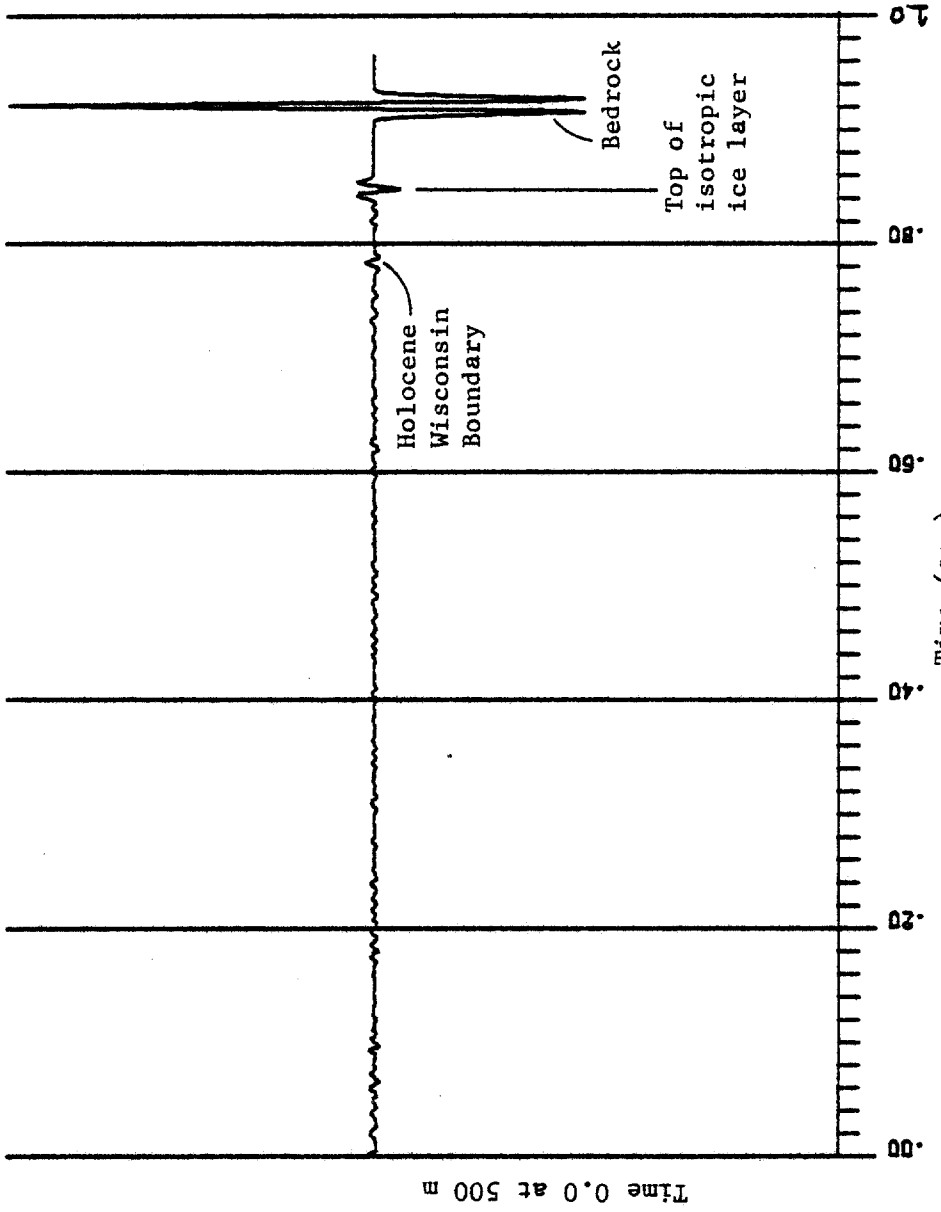

Figure 12. Synthetic Seismogram with isotropic ice layer

6. COMPARISON WITH LOGGING AT BYRD STATION, ANTARCTICA

Bentley (1972) conducted sonic logging at Byrd Station, Antarctica, with the same borehole unit that was used at Dye-3. The Byrd hole (2164 m) was completed to bedrock; unfortunately, only the top 1550 m could be logged because of drilling debris blocking the hole. Figure 13 shows a comparison of the Byrd Station and Dye-3 data. It is important to note that the velocities are plotted vs. depth; if plotted vs. time the Byrd data would be expanded. Unfortunately the depth vs. time relationship is not yet available for Dye-3 so a detailed comparison on a time basis is not possible.

The portion of the Dye-3 curve at depths less than 100 m which is characterized by a rapid velocity change with respect to depth was not obtained at Byrd due to casing in the hole.

Between 250 and 400 m the Byrd velocities are 25-40 m/s faster than the Dye-3 velocities. This portion of the ice sheet is considered to be isotropic at both sites. The temperature at Dye-3 is 7.5-8.0°C warmer than at Byrd in this region (Ueda, 1968; Gundestrup, personal communication, 1982). This can account for about 17 m/s difference in the velocities. Another effect is necessary to account for the remainder. An unrealistically large density difference of .006 g/cm^3 would be required to account for a 20 m/s difference (Bennett, 1968). Experimental error could also account for a 20 m/s difference.

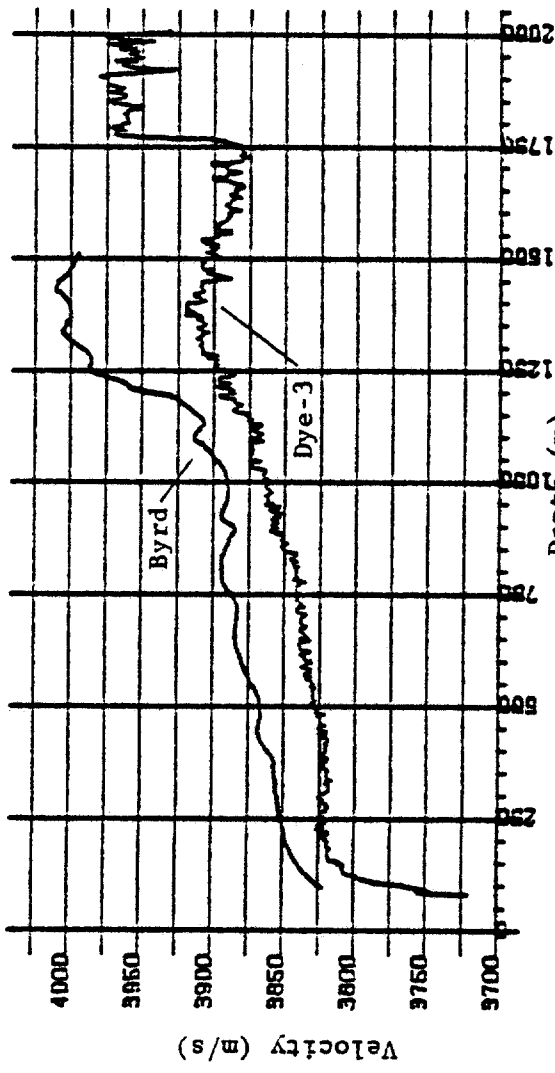

Figure 13. Vertival P Wave Velocity vs. Depth at Dye-3, Greenland and Byrd Station, Antartica

Starting at 400 m the effects of anisotropic ice are noticeable at both sites. The temperature difference between the sites, and hence the temperature-induced velocity difference, decreases until at 650 m the two temperatures are the same. The velocity difference between sites in this region is probably caused by a higher level of anisotropy at any given depth at Byrd than at Dye-3.

The Holocene-Wisconsin boundary at Byrd (1200 m) is not as sharply defined as at Dye-3. The gradual hump in the velocity curve at 1300 m at Dye-3 is not present at Byrd. The greater depth of the Holocene-Wisconsin boundary at Dye-3 is the result of a higher accumulation rate at Dye-3 of 0.53 m ice/year (Whillans, personal communication, 1982) as compared to Byrd, 0.17 m ice/year (Gow, 1971).

The time represented by the transition in the Byrd core is on the order of 10,000 years (Dansgaard, et al., 1968). Because the transition occurs at a greater depth in the Dye-3 core, the time scale is more compacted with respect to depth and it is possible that the same time interval is represented at Dye-3. The oxygen isotope analysis which can determine this is not yet available.

If the Byrd velocity curve is expanded so that the Holocene-Wisconsin boundary occurs at the same depth as at Dye-3, the velocity difference between the sites will be reduced. It is likely that the velocity at 1350 m at Dye-3 will be higher than the corresponding expanded Byrd velocities. The key issue in choosing a comparison method is knowing to what extent the fabric, and hence velocity, is a function of time and depth.

7. COMPARISON TO CORE ANALYSIS

The Dye-3 core has been extensively analyzed by Herron, et al. (1982). Vertical and horizontal velocities as well as fabrics were investigated. Their analysis puts the Holocene-Wisconsin boundary at 1778 m vs. 1767 m as determined by logging; the 11 m difference may be the result of different zero-depth datum levels.

Figure 14 shows a comparison of Herron's measured vertical and horizontal velocities to the logged vertical and calculated horizontal velocities. All velocities are corrected to a temperature of -10°C. The uncertainty for the logged values is 5 m/s and for the core measurements 30 m/s. The methods agree to within the expected error. This is particularly significant for the calculated horizontal velocities which are calculated from Bennett's (1972) work on wave propagation in crystal aggregates. Although Bennett's work assumes only an evenly-distributed conical distribution of c axes, this is clearly a valid approximation for determining relative velocities on the large scale of logger measurements.

Figure 15 shows a comparison of calculated fabric vs. Herron's measured fabric. The general trend toward a tighter distribution with depth is supported by both methods. There is, however, a shift of 5°-15° between the methods. Herron's fabric parameter is the angle of a cone which contains 90% of the

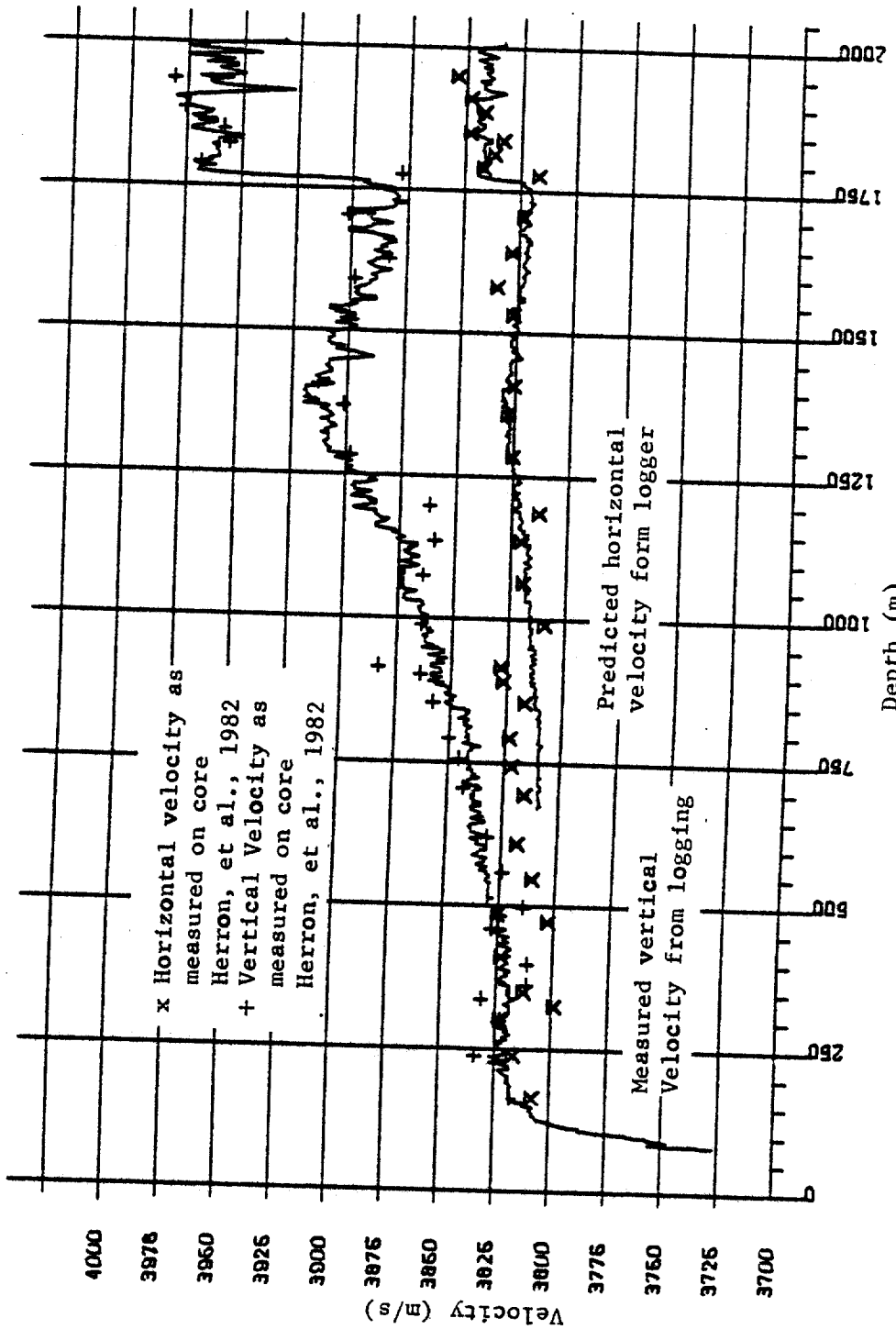

Figure 14. Comparison of logger and core results

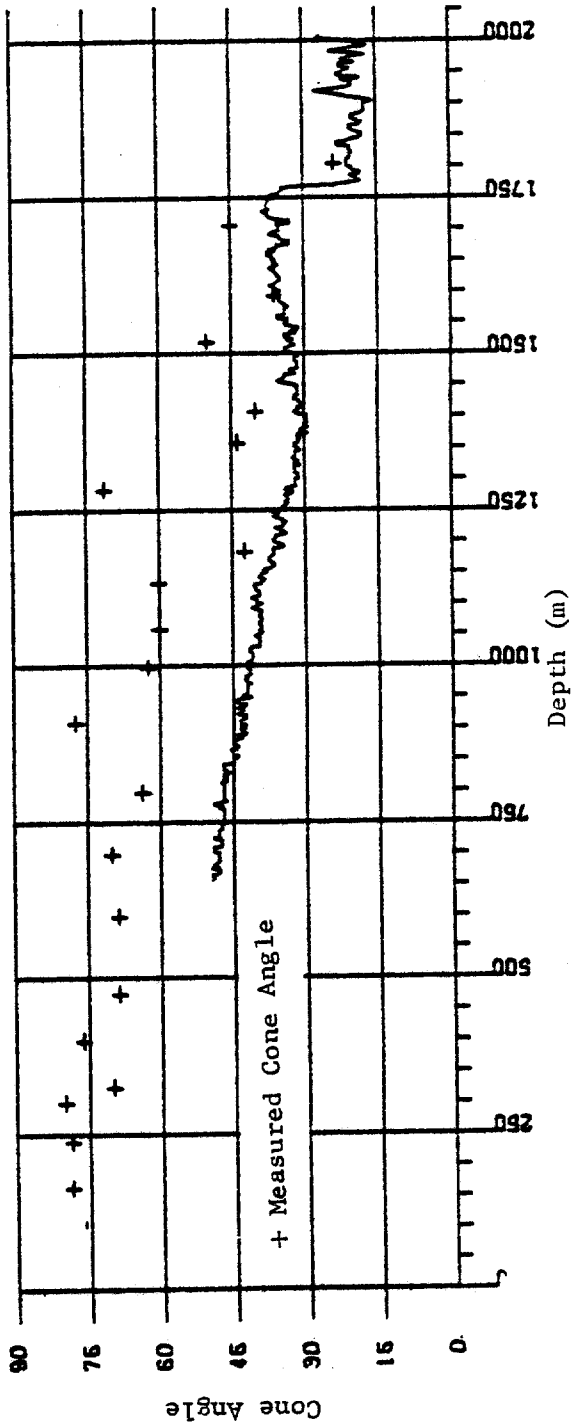

Figure 15. Calculated vs. Measured Cone Angle.

c axes, regardless of the distribution in the cone. The predicted fabric parameter is based on Bennett's assumption of all axes being evenly distributed thoughout a cone. This will result in a smaller calculated cone angle than Herron's measured cone angle.

In Figure 16 the vertical velocity as measured by logging and core measurements are compared with the velocity that is obtained by applying Bennett's relationship for a solid cone to Herron's fabric analysis. The 53 m/s difference between Bennett's theoretical value for the P-wave velocity in isotropic ice and Kohnen's measured value was subtracted from the calculated velocities. This is consistent with the method used to compute the calculated fabric from velocities in Section 5.2. Above 1100 m the calculated values are smooth but have a slope different from either set of measured values. This is a result of the increased error of Bennett's assumption, of a cone containing 90% of the c axis, at intermediate cone angles. Below 1100 m the calculated values have a large scatter which demonstrates the local nature of thin section analysis.

By a depth of 1200 m air bubbles within the ice are compressed to the extent that they are no longer visually detectable. This depth also marks a downward increase in the velocity gradient. Herron suggests the absence of bubbles as a possible cause of the velocity increase.

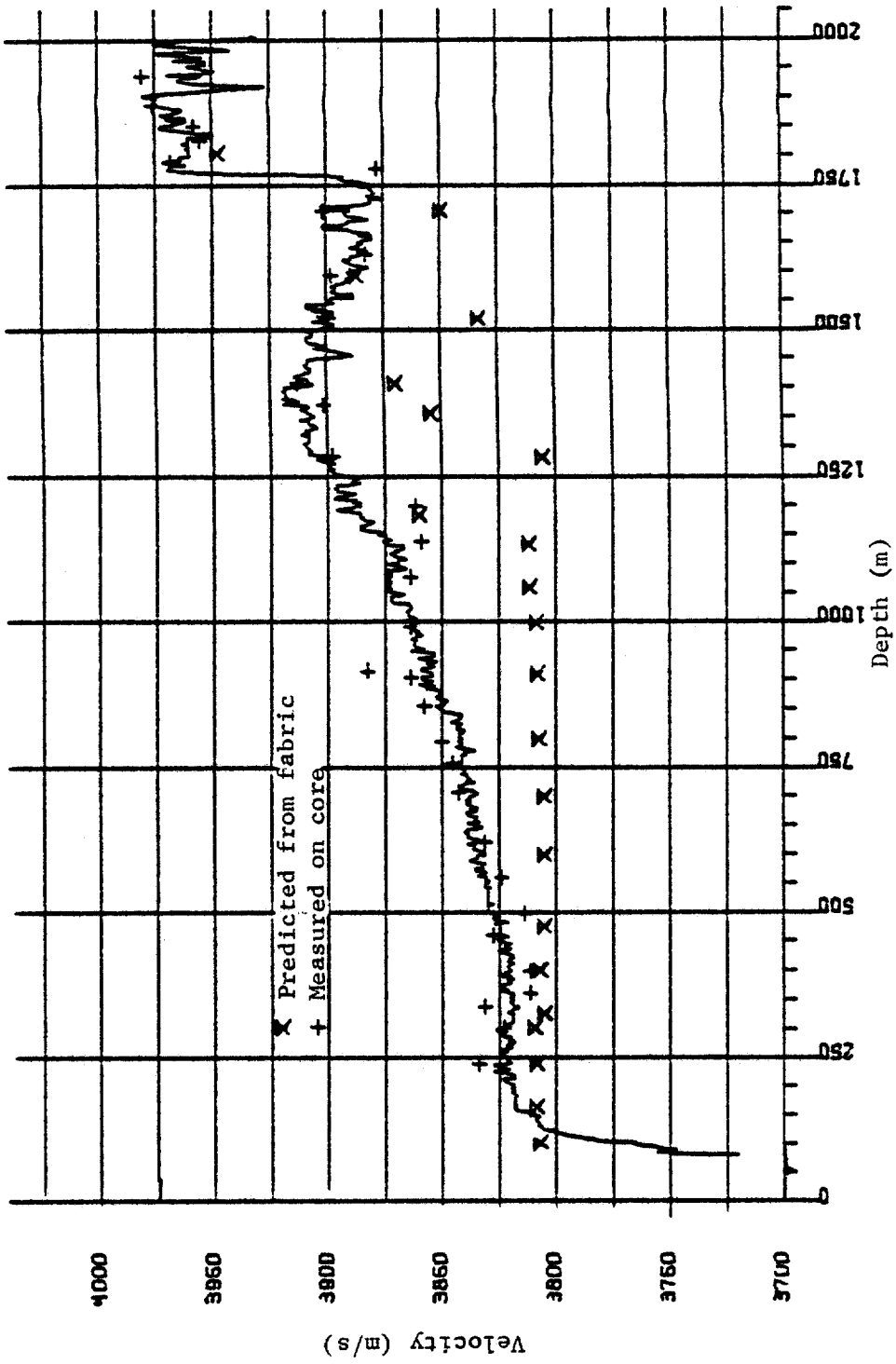

Figure 16. Predicted vs. Measured Vertical Velocity.

The cause of the decrease below 1400 m is still unknown.

Herron reports that the crystal size ranges from 0.2-0.6 cm above the Holocene-Wisconsin boundary, and decreases sharply to 0.05-0.2 cm below the boundary. These sizes are sufficiently small, compared to the 15-cm wavelength of the signal transmitted by the logger, to exclude the possibility of crystal size effecting the logging measurements.

8. CONCLUSIONS

Sonic logging of ice sheets is a powerful technique for the investigation of crystal fabric. This can be particularly useful when the drilling method does not yield a core.

Waveform studies show no significant changes in amplitude or waveform received with depth. Crystal fabrics can be estimated using Bennett's (1972) relationship for the dependence of wave velocity on crystal fabrics. The estimated fabrics can be used to predict a velocity for P-waves traveling perpendicular to the borehole. Comparison of the predicted velocities with those measured on the core shows excellent agreement. The Holocene-Wisconsin boundary is clearly observed by logging. There is also a change in velocity gradient occurring at the depth of bubble disappearance. Synthetic seismograms support the belief that detection of the Holocene-Wisconsin boundary by surface seismic reflection methods would be extremely difficult. Due to the existence of layers of nearly equal horizontal velocity, surface refraction methods would also have difficulty locating the Holocene-Wisconsin boundary. The abrupt change in character 150 m above bedrock is suggested as evidence for a basal deformation zone. The Dye-3 velocity profile is very similar to the Byrd Station velocity profile.

9. SUMMARY

1. The improved version of the University of Wisconsin logging system is capable of measuring P-wave velocities with a relative error of less than 5 m/s, i.e. about 0.1%. It also maintains waveform and amplitude information.

2. Measured vertical P-wave velocities at Dye-3 reach a maximum of 3990 m/s at 1850 m.

3. An abrupt change in vertical P-wave velocity of 75 m/s occurs over less than a 7-m interval starting at 1767 m. This represents the Holocene Wisconsin boundary.

4. The ice fabric can be modeled by a uniform distribution of c-axes in a solid vertically-oriented cone with an apex angle ranging from 50° at 500 m to 20° below 1770 m. This is in general agreement with the core analysis.

5. Horizontal P-wave velocities are calculated to range from 3805 m/s at 700 m to 3820 m/s at 1750 m.

6. The vertical and horizontal P-wave velocities obtained by sonic logging and core work agree to within experimental error.

7. Internal reflections in the ice would have amplitudes 0.14 to 0.02 times the amplitude of the bottom reflection which could explain some, but not all, of the pre-bedrock reflections noted by Bentley (1971).

REFERENCES

Bennett, H.F., 1972. Measurements of ultrasonic wave velocities in ice cores from Greenland and Antarctica. U.S. Army CRREL Research Report #237.

Bennett, H.F., 1968. An investigation into velocity anisotropy through measurements of ultrasonic wave velocities in snow and ice cores from Greenland and Antarctica. Ph.D. Thesis, University of Wisconsin.

Bentley, C.R., 1977. Impurities and seismic wave attenuation in the West Antarctic ice sheet. Symposium on Isotopes and Impurities in Snow and Ice, IAHS Publication No. 118, p. 13-16.

Bentley, C.R., 1972. Seismic wave velocities in anisotropic ice: A comparison of measured and calculated values in and around the deep drill hole at Byrd Station, Antarctica. J. Geophysical Research, vol. 77, no. 23, p. 4406-4420.

Bentley, C.R., 1971. Seismic evidence for moraine within the basal Antarctic ice sheet. American Geophysical Union, Antarctic Research Series, vol. 16, p. 89-129.

Bentley, C.R., 1971. Seismic anisotropy of the West Antarctic ice sheet. American Geophysical Union, Antarctic Research Series, vol. 16, p. 131-177.

Dansgaard, W., and N. Reeh, 1982. Climatic interpretation of GISP ice core data. EOS, Trans. Am. Geophys. Union, vol. 63, no. 18, p. 298.

Dansgaard, W., S.J. Johnsen, J. Moller, and C.C. Langway, 1968. Oxygen isotope analysis of a core representing a complete vertical profile of a polar ice sheet. International Symposium on Antarctic Glaciological Exploration (ISAGE), p. 93-94.

Gow, A.T., 1971. Depth-time-temperature relationships of ice crystal growth in polar glaciers. U.S. Army CRREL, Research Report No. 330.

Herron, S.L., C.C. Langway, and K.A. Brugger, 1982. Ultrasonic velocities and crystalline anisotropy in the ice core from Dye-3, Greenland. J. Glaciology, in press.

Kohnen, H., 1974. The temperature dependence of seismic waves in ice. J. Glaciology, vol. 13, no. 67, p. 144-148.

Ueda, H.T., and D.E. Garfield, 1968. Deep core drilling at Byrd Station, Antarctica. International Symposium on Antarctic Glaciological Exploration (ISAGE), p. 53-62.

APPENDIX 1

SURFACE ELECTRONICS - THEORY OF OPERATION

This is a brief description of how the equipment worked in the field. At the time of this writing, the equipment is being modified to reduce its logic to a simpler form. A complete description will be written when this is completed.

The sync signal passes through a CMR transformer and is shaped before entering the OR gate (13). Either the sync or the restore switch will pulse the flip-flop (10). The sync also resets counter 9 which generates the 100-kHz signal for the counters.

The output of the flip-flop (10) starts either the A or B set of cascaded counters. The counter outputs are combined at AND gate (12). This pulse is conditioned to be the sync out. It also presets the counters.

The amplifier uses a digital-to-analog device (15) to control the feedback on Op-Amp (14). The counter start line determines which rotary switch (18) will control the D-A device.

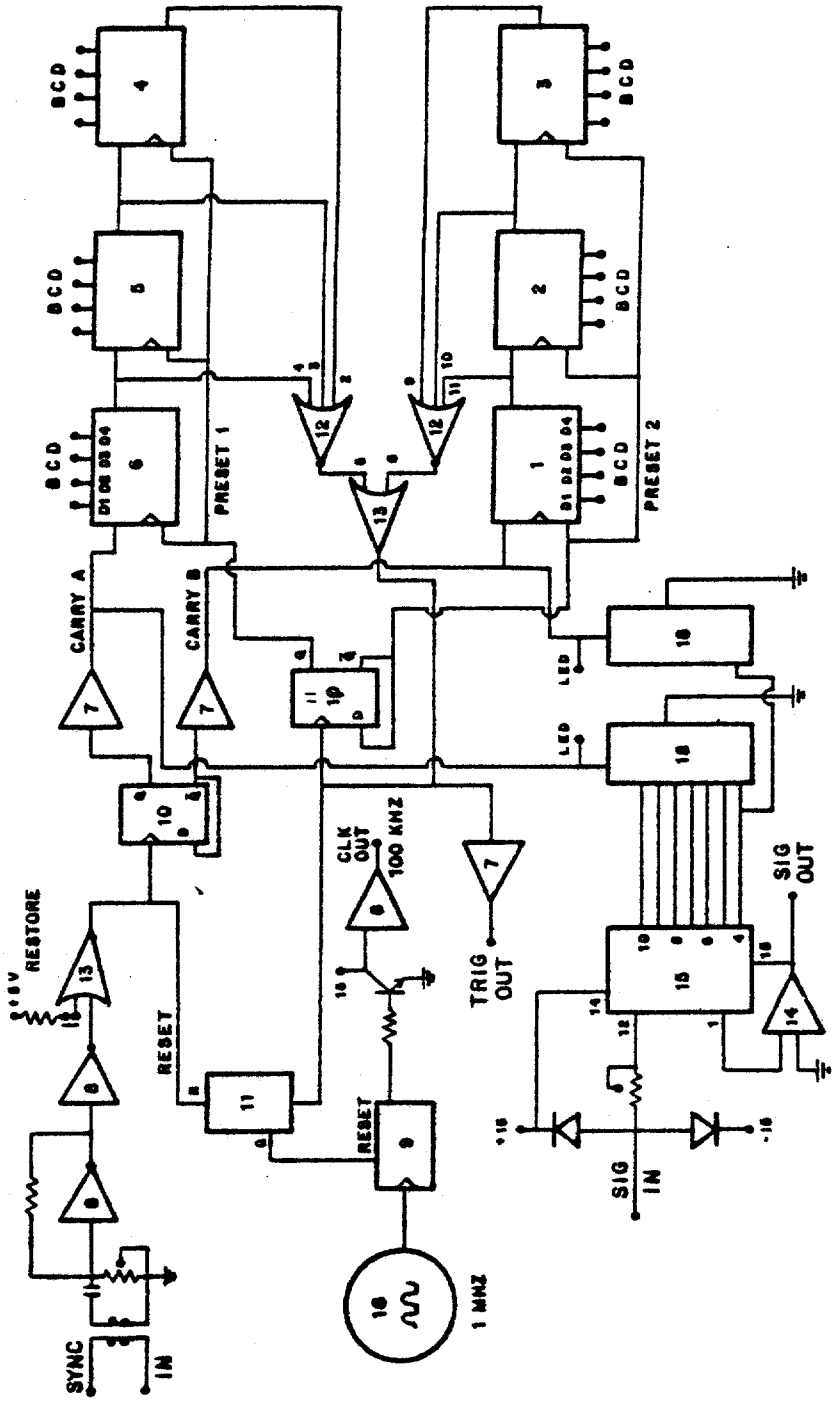

Figure 17. Surface Electronics Schematic.

IC Packages

Z1 - Z6	MC 14510	BCD presettable up/down counter
Z7	MC 14050B	Hex Buffers
Z8	MC 14049 UB	Hex Inverters
Z9	MC 14520B	Dual BCD up/down counter
Z10	MC 14013B	Dual D flip-flop
Z11	MC 14013B	Dual D flip-flop
Z12	MC 14002B	Dual 4 input Nor gates
Z13	MC 14071B	Quad 2 input orgates
Z14	PMI OP-27	Precision op amp
Z15	AD 7520	Analog devices multiplying D/A converter
Z16	TCXO CO252-3A	1MHz vection crystal oscillator
Z17	7805	Positive 5 V regulator
Z18	-	12-position rotary switch

APPENDIX 2

CALCULATION OF CABLE STRETCH

Gerhardt Owen Inc. of Fort Worth, Texas, provided the information on the cable.

δ = linear density in water = 0.2 (Kg/m)

E = elongation (E) = $2.4 \times 10^{-6} \left(\frac{\Delta L}{L\ Kg}\right)$ $E = 2.4 \times 10^{-6}\ Kg^{-1}$

To calculate the stretch we let

F = force on cable (Kg)

z = distance above logger (m)

The mass of the logger is approximately 90 Kg

$F = g\ \delta\ z + 90$

The stretch over an interval Δz is $S_i = E\ F\ \Delta\ z$

The total stretch is the integral of the interval stretches

$$S_t = \int_{z_o}^{z_1} E\ F\ d\ z$$

$$= E \int_{z_o}^{z_1} (g\ \delta\ z + 90)\ dz$$

$$= E\left(g\frac{\delta}{2}z^2 + 90\ z\right) \Big/_{z_o}^{z_1}$$

$$= 2.4 \times 10^{-7}\ z^2 + 2.2 \times 10^{-4}\ z$$

At 2000 m the stretch is 1.4 m.

APPENDIX 3

Tabulation of Vertical P-Wave Velocity vs. Depth

DEPTH	VELOCITY	DEPTH	VELOCITY	DEPTH	VELOCITY
80. 42	3744. 52	214. 57	3842. 25	348. 73	3842. 25
83. 46	3769. 76	217. 62	3842. 25	351. 78	3843. 31
86. 51	3779. 95	220. 67	3843. 31	354. 83	3842. 25
89. 56	3771. 79	223. 71	3847. 54	357. 88	3842. 25
92. 61	3777. 90	226. 76	3850. 72	360. 93	3843. 31
95. 66	3780. 97	229. 81	3844. 37	363. 97	3846. 48
98. 71	3788. 14	232. 86	3847. 54	367. 02	3844. 37
101. 76	3790. 19	235. 91	3850. 72	370. 07	3847. 54
104. 81	3802. 56	238. 96	3846. 48	373. 12	3846. 48
107. 85	3810. 85	242. 01	3843. 31	376. 17	3845. 42
110. 90	3810. 85	245. 06	3844. 37	379. 22	3843. 31
113. 95	3817. 09	248. 11	3844. 37	382. 27	3844. 37
117. 00	3820. 21	251. 16	3846. 48	385. 32	3842. 25
120. 05	3822. 30	254. 20	3846. 48	388. 37	3843. 31
123. 10	3825. 44	257. 25	3847. 54	391. 42	3847. 54
126. 15	3829. 63	260. 30	3845. 42	394. 47	3845. 42
129. 20	3830. 68	263. 35	3847. 54	397. 52	3844. 37
132. 25	3831. 73	266. 40	3843. 31	400. 57	3843. 31
135. 29	3831. 73	269. 45	3845. 42	403. 62	3844. 37
138. 34	3831. 73	272. 50	3843. 31	406. 66	3844. 37
141. 39	3832. 78	275. 55	3842. 25	409. 71	3843. 31
144. 44	3832. 78	278. 60	3844. 37	412. 76	3842. 25
147. 49	3831. 73	281. 65	3843. 31	415. 81	3844. 37
150. 54	3835. 93	284. 70	3843. 31	418. 86	3843. 31
153. 59	3833. 83	287. 74	3847. 54	421. 91	3842. 25
156. 64	3838. 04	290. 79	3847. 54	424. 96	3842. 25
159. 69	3841. 20	293. 84	3845. 42	428. 01	3843. 31
162. 73	3842. 25	296. 89	3849. 66	431. 06	3847. 54
165. 78	3842. 25	299. 94	3847. 54	434. 11	3847. 54
168. 83	3842. 25	302. 99	3845. 42	437. 16	3843. 31
171. 88	3842. 25	306. 04	3845. 42	440. 21	3845. 42
174. 93	3842. 25	309. 09	3843. 31	443. 26	3844. 37
177. 98	3842. 25	312. 14	3842. 25	446. 31	3843. 31
181. 03	3842. 25	315. 19	3842. 25	449. 36	3847. 54
184. 08	3841. 20	318. 24	3842. 25	452. 41	3848. 60
187. 13	3842. 25	321. 29	3842. 25	455. 45	3846. 48
190. 18	3843. 31	324. 33	3842. 25	458. 50	3844. 37
193. 22	3842. 25	327. 38	3844. 37	461. 55	3847. 54
196. 27	3843. 31	330. 43	3843. 31	464. 60	3847. 54
199. 32	3842. 25	333. 48	3842. 25	467. 65	3847. 54
202. 37	3842. 25	336. 53	3840. 14	470. 70	3847. 54
205. 42	3844. 37	339. 58	3842. 25	473. 75	3847. 54
208. 47	3845. 42	342. 63	3842. 25	476. 80	3847. 54
211. 52	3846. 48	345. 68	3843. 31	479. 85	3849. 66

DEPTH	VELOCITY	DEPTH	VELOCITY	DEPTH	VELOCITY
482. 90	3844. 37	617. 08	3861. 35	751. 27	3863. 48
485. 95	3847. 54	620. 13	3858. 15	754. 32	3863. 48
489. 00	3850. 72	623. 18	3854. 96	757. 37	3863. 48
492. 05	3848. 60	626. 23	3858. 15	760. 42	3863. 48
495. 10	3850. 72	629. 28	3861. 35	763. 47	3863. 48
498. 15	3850. 72	632. 33	3861. 35	766. 52	3863. 48
501. 20	3852. 84	635. 38	3861. 35	769. 57	3863. 48
504. 25	3852. 84	638. 43	3862. 41	772. 62	3861. 35
507. 30	3852. 84	641. 48	3861. 35	775. 67	3862. 41
510. 34	3852. 84	644. 53	3858. 15	778. 72	3858. 15
513. 39	3850. 72	647. 58	3854. 96	781. 77	3862. 41
516. 44	3852. 84	650. 63	3858. 15	784. 82	3865. 62
519. 49	3852. 84	653. 68	3861. 35	787. 87	3863. 48
522. 54	3852. 84	656. 73	3856. 02	790. 92	3863. 48
525. 59	3852. 84	659. 78	3858. 15	793. 97	3864. 55
528. 64	3852. 84	662. 83	3857. 09	797. 02	3864. 55
531. 69	3852. 84	665. 87	3859. 22	800. 07	3863. 48
534. 74	3852. 84	668. 92	3861. 35	803. 12	3864. 55
537. 79	3852. 84	671. 97	3861. 35	806. 17	3864. 55
540. 84	3851. 78	675. 02	3857. 09	809. 22	3863. 48
543. 89	3853. 90	678. 07	3860. 28	812. 27	3862. 41
546. 94	3853. 90	681. 12	3857. 09	815. 32	3865. 62
549. 99	3852. 84	684. 17	3860. 28	818. 37	3864. 55
553. 04	3852. 84	687. 22	3861. 35	821. 42	3865. 62
556. 09	3853. 90	690. 27	3860. 28	824. 47	3863. 48
559. 14	3853. 90	693. 32	3861. 35	827. 52	3867. 75
562. 19	3857. 09	696. 37	3860. 28	830. 57	3865. 62
565. 24	3854. 96	699. 42	3860. 28	833. 62	3864. 55
568. 29	3853. 90	702. 47	3858. 15	836. 67	3863. 48
571. 34	3858. 15	705. 52	3857. 09	839. 72	3863. 48
574. 38	3858. 15	708. 57	3858. 15	842. 77	3865. 62
577. 43	3854. 96	711. 62	3862. 41	845. 82	3870. 97
580. 48	3854. 96	714. 67	3863. 48	848. 87	3872. 04
583. 53	3853. 90	717. 72	3863. 48	851. 92	3873. 11
586. 58	3857. 09	720. 77	3862. 41	854. 97	3874. 18
589. 63	3860. 28	723. 82	3858. 15	858. 02	3870. 97
592. 68	3858. 15	726. 87	3861. 35	861. 07	3872. 04
595. 73	3857. 09	729. 92	3860. 28	864. 12	3869. 90
598. 78	3853. 90	732. 97	3861. 35	867. 17	3873. 11
601. 83	3853. 90	736. 02	3861. 35	870. 22	3874. 18
604. 88	3854. 96	739. 07	3863. 48	873. 27	3873. 11
607. 93	3859. 22	742. 12	3862. 41	876. 32	3872. 04
610. 98	3858. 15	745. 17	3862. 41	879. 37	3872. 04
614. 03	3858. 15	748. 22	3863. 48	882. 42	3874. 18

DEPTH	VELOCITY	DEPTH	VELOCITY	DEPTH	VELOCITY
885. 47	3878. 48	1019. 68	3886. 02	1153. 90	3897. 94
888. 52	3875. 26	1022. 73	3884. 94	1156. 95	3904. 47
891. 57	3881. 71	1025. 78	3884. 94	1160. 00	3906. 65
894. 62	3878. 48	1028. 83	3886. 02	1163. 05	3906. 65
897. 67	3876. 33	1031. 88	3892. 51	1166. 10	3904. 47
900. 72	3880. 63	1034. 93	3893. 60	1169. 15	3902. 29
903. 77	3880. 63	1037. 98	3893. 60	1172. 20	3901. 20
906. 82	3876. 33	1041. 03	3893. 60	1175. 25	3904. 47
909. 87	3876. 33	1044. 08	3892. 51	1178. 30	3905. 56
912. 92	3876. 33	1047. 13	3888. 18	1181. 35	3906. 65
915. 97	3880. 63	1050. 18	3893. 60	1184. 40	3906. 65
919. 02	3880. 63	1053. 23	3894. 68	1187. 45	3906. 65
922. 07	3875. 26	1056. 28	3893. 60	1190. 50	3915. 40
925. 12	3876. 33	1059. 33	3894. 68	1193. 55	3916. 49
928. 17	3878. 48	1062. 38	3895. 77	1196. 60	3912. 11
931. 22	3874. 18	1065. 43	3893. 60	1199. 65	3906. 65
934. 27	3879. 56	1068. 48	3893. 60	1202. 70	3906. 65
937. 32	3881. 71	1071. 53	3895. 77	1205. 76	3909. 93
940. 37	3875. 26	1074. 58	3895. 77	1208. 81	3908. 83
943. 42	3875. 26	1077. 63	3893. 60	1211. 86	3917. 59
946. 47	3877. 41	1080. 68	3893. 60	1214. 91	3916. 49
949. 52	3884. 94	1083. 74	3895. 77	1217. 96	3912. 11
952. 57	3879. 56	1086. 79	3894. 68	1221. 01	3908. 83
955. 62	3882. 79	1089. 84	3890. 35	1224. 06	3916. 49
958. 67	3883. 87	1092. 89	3887. 10	1227. 11	3916. 49
961. 72	3883. 87	1095. 94	3890. 35	1230. 16	3917. 59
964. 77	3883. 87	1098. 99	3894. 68	1233. 21	3916. 49
967. 82	3882. 79	1102. 04	3890. 35	1236. 26	3909. 93
970. 87	3884. 94	1105. 09	3890. 35	1239. 31	3906. 65
973. 92	3882. 79	1108. 14	3887. 10	1242. 36	3909. 93
976. 97	3880. 63	1111. 19	3889. 27	1245. 41	3908. 83
980. 02	3882. 79	1114. 24	3892. 51	1248. 46	3906. 65
983. 07	3881. 71	1117. 29	3893. 60	1251. 52	3913. 21
986. 12	3883. 87	1120. 34	3890. 35	1254. 57	3916. 49
989. 17	3884. 94	1123. 39	3891. 43	1257. 62	3918. 69
992. 22	3883. 87	1126. 44	3888. 18	1260. 67	3919. 79
995. 28	3882. 79	1129. 49	3888. 18	1263. 72	3917. 59
998. 33	3884. 94	1132. 54	3894. 68	1266. 77	3920. 89
1001. 38	3887. 10	1135. 59	3895. 77	1269. 82	3919. 79
1004. 43	3882. 79	1138. 64	3896. 85	1272. 87	3917. 59
1007. 48	3883. 87	1141. 69	3893. 60	1275. 92	3921. 99
1010. 53	3886. 02	1144. 74	3895. 77	1278. 97	3925. 29
1013. 58	3886. 02	1147. 79	3895. 77	1282. 02	3917. 59
1016. 63	3887. 10	1150. 85	3899. 02	1285. 07	3919. 79

DEPTH	VELOCITY	DEPTH	VELOCITY	DEPTH	VELOCITY
1288. 12	3928. 60	1422. 36	3931. 91	1562. 71	3915. 40
1291. 17	3928. 60	1425. 41	3929. 70	1565. 76	3916. 49
1294. 23	3927. 49	1428. 46	3927. 49	1568. 81	3915. 40
1297. 28	3928. 60	1431. 51	3927. 49	1571. 86	3915. 40
1300. 33	3929. 70	1434. 56	3928. 60	1574. 91	3916. 49
1303. 38	3929. 70	1437. 62	3929. 70	1577. 97	3914. 30
1306. 43	3930. 80	1440. 67	3928. 60	1581. 02	3912. 11
1309. 48	3928. 60	1443. 72	3928. 60	1584. 07	3909. 93
1312. 53	3928. 60	1446. 77	3928. 60	1587. 12	3909. 93
1315. 58	3928. 60	1449. 82	3925. 29	1590. 17	3907. 74
1318. 63	3928. 60	1452. 87	3916. 49	1593. 22	3906. 65
1321. 68	3931. 91	1455. 92	3908. 83	1596. 27	3906. 65
1324. 73	3928. 60	1462. 02	3915. 40	1599. 32	3908. 83
1327. 78	3929. 70	1465. 07	3917. 59	1605. 43	3904. 47
1330. 83	3927. 49	1468. 13	3925. 29	1608. 48	3900. 11
1333. 89	3925. 29	1471. 18	3924. 19	1611. 53	3905. 56
1336. 94	3926. 39	1474. 23	3921. 99	1614. 58	3907. 74
1339. 99	3928. 60	1477. 28	3927. 49	1617. 63	3908. 83
1343. 04	3928. 60	1480. 33	3928. 60	1620. 68	3909. 93
1346. 09	3931. 91	1483. 38	3928. 60	1623. 73	3906. 65
1349. 14	3928. 60	1486. 43	3928. 60	1626. 79	3906. 65
1352. 19	3926. 39	1489. 48	3926. 39	1629. 84	3903. 38
1355. 24	3927. 49	1492. 53	3926. 39	1632. 89	3903. 38
1358. 29	3928. 60	1495. 59	3927. 49	1635. 94	3899. 02
1361. 34	3929. 70	1498. 64	3928. 60	1638. 99	3901. 20
1364. 39	3931. 91	1501. 69	3923. 09	1642. 04	3906. 65
1367. 44	3928. 60	1504. 74	3917. 59	1645. 09	3903. 38
1370. 50	3929. 70	1507. 79	3917. 59	1648. 15	3901. 20
1373. 55	3939. 66	1510. 84	3918. 69	1651. 20	3903. 38
1376. 60	3933. 02	1513. 89	3926. 39	1654. 25	3901. 20
1379. 65	3934. 12	1519. 99	3918. 69	1657. 30	3896. 85
1382. 70	3939. 66	1523. 05	3924. 19	1660. 35	3896. 85
1385. 75	3937. 44	1526. 10	3917. 59	1663. 40	3902. 29
1388. 80	3938. 55	1529. 15	3917. 59	1666. 45	3897. 94
1391. 85	3938. 55	1532. 20	3926. 39	1669. 50	3904. 47
1394. 90	3939. 66	1535. 25	3921. 99	1672. 56	3906. 65
1397. 95	3938. 55	1538. 30	3928. 60	1675. 61	3917. 59
1401. 00	3938. 55	1541. 35	3928. 60	1678. 66	3917. 59
1404. 06	3929. 70	1544. 40	3920. 89	1681. 71	3908. 83
1407. 11	3926. 39	1547. 45	3916. 49	1684. 76	3906. 65
1410. 16	3928. 60	1550. 50	3918. 69	1687. 81	3906. 65
1413. 21	3928. 60	1553. 56	3917. 59	1690. 86	3897. 94
1416. 26	3933. 02	1556. 61	3907. 74	1693. 92	3901. 20
1419. 31	3934. 12	1559. 66	3907. 74	1696. 97	3906. 65

DEPTH	VELOCITY	DEPTH	VELOCITY	DEPTH	VELOCITY
1700. 02	3907. 74	1834. 28	3963. 11	1977. 72	3983. 42
1703. 07	3907. 74	1837. 34	3961. 98	1980. 77	3973. 24
1706. 12	3905. 56	1840. 39	3968. 73	1983. 82	3950. 79
1709. 17	3917. 59	1843. 44	3974. 37	1986. 87	3960. 86
1712. 22	3917. 59	1846. 49	3982. 29	1989. 92	3976. 63
1715. 27	3901. 20	1849. 54	3984. 56	1992. 97	3983. 42
1718. 33	3896. 85	1852. 59	3983. 42	1996. 03	3974. 37
1721. 38	3895. 77	1855. 65	3978. 89	1999. 08	3973. 24
1724. 43	3895. 77	1858. 70	3974. 37	2002. 13	3950. 79
1727. 48	3890. 35	1861. 75	3973. 24	2005. 18	3938. 55
1730. 53	3896. 85	1864. 80	3973. 24	2008. 23	3939. 66
1733. 58	3894. 68	1867. 85	3981. 16		
1736. 63	3893. 60	1870. 90	3983. 42		
1739. 69	3894. 68	1873. 96	3978. 89		
1742. 74	3895. 77	1877. 01	3975. 50		
1745. 79	3895. 77	1880. 06	3974. 37		
1748. 84	3900. 11	1883. 11	3978. 89		
1751. 89	3895. 77	1886. 16	3982. 29		
1754. 94	3900. 11	1889. 21	3984. 56		
1758. 00	3906. 65	1892. 27	3984. 56		
1761. 05	3908. 83	1898. 37	3984. 56		
1764. 10	3906. 65	1901. 42	3984. 56		
1767. 15	3917. 59	1904. 47	3990. 24		
1770. 20	3956. 38	1907. 52	3984. 56		
1773. 25	3974. 37	1910. 58	3973. 24		
1776. 30	3983. 42	1913. 63	3963. 11		
1779. 36	3982. 29	1916. 68	3950. 79		
1782. 41	3982. 29	1919. 73	3937. 44		
1785. 46	3975. 50	1922. 78	3950. 79		
1788. 51	3983. 42	1925. 84	3967. 60		
1791. 56	3984. 56	1928. 89	3973. 24		
1794. 61	3976. 63	1931. 94	3974. 37		
1797. 67	3977. 76	1934. 99	3973. 24		
1800. 72	3973. 24	1938. 04	3964. 23		
1803. 77	3973. 24	1941. 09	3978. 89		
1806. 82	3973. 24	1944. 15	3964. 23		
1809. 87	3973. 24	1947. 20	3958. 62		
1812. 92	3974. 37	1956. 35	3969. 86		
1815. 97	3973. 24	1959. 40	3961. 98		
1819. 03	3973. 24	1962. 46	3961. 98		
1822. 08	3975. 50	1965. 51	3975. 50		
1825. 13	3973. 24	1968. 56	3967. 60		
1828. 18	3973. 24	1971. 61	3963. 11		
1831. 23	3973. 24	1974. 66	3973. 24		

APPENDIX 4

PROGRAM FOR CALCULATING SEISMIC REFLECTION COEFFICIENTS

This program is for reducing sonic logger data and for calculating reflection coefficients from a log of depth vs. impedence.

DM1, Dm2 = Depth in meters to the top and bottom of the layer, respectively.

Q1 = Impedence of layer.

Z = Thickness of layer in kilometers.

RD = Reflection coefficient for a downward-traveling wave.

TD = Transmission coefficient for a downward-traveling wave.

RU = Reflection coefficient for an upward-traveling wave.

TU = Transmission coefficient for an upward-traveling wave.

ATL = The attenuation in the layer.

AD = Amplitude of downward traveling wave.

UA = The attenuation of an upward-traveling wave moving from the layer to the surface.

REFCOF = The reflection coefficient.

```
 CALL LINK
 OPEN #
 OPEN $
 AD=1
 UAT=1

 READ(3,100) DM1,Q1,D1,D2,D3
 FORMAT (5F10.2)
 READ (3,100) DM2,Q2,D1,D2,D3
 IF (DM2.GT.2650) STOP
 Z=(DM2-DM1)/1000
 RD=(Q1-Q2)/(Q1+Q2)
 TD=(1-RD*RD)**.5
 RU=(Q2-Q1)/(Q1+Q2)
 TU=(1-RU*RU)**.5
 ATL=(2.718**(-.155*z))*((DM1-z)/DM1)
 AD=AD*TD*ATL
 UAT=UAT*TU*ATL
 REFCOF=AD*RD*UAT
WRITE (4,300) DM2,REFCOF
FORMAT (2G20.4)
Q1=Q2
DM1=DM2
GO TO 200
END
```

APPENDIX 5

SUGGESTED EQUIPMENT IMPROVEMENTS

The new surface unit worked very well once it was debugged. The schematic shown in Appendix 1 is the circuit that was used to record the data presented here. Some component modifications are being made to reduce the logic to a simpler state. (The revised schematic will be with the equipment.) The biggest problem is grounding noise. The borehole unit (BHU) design uses the cable armor as a ground return. It implies that the ground potential at the BHU is the same as at the surface and the same at the equipment ground. When this is not the case, as at Dye-3, there are currents set up in the ground lines. Unfortunately, the receiver signals also use the ground line, and hence pick up noise. A reasonable solution would be to send the received signals up in common mode form. It might also help to isolate the BHU ground from the housing, but this would be more difficult and not as effective.

Fortunately, the Dye-3 hole was smooth. In an irregular hole travel times will be affected greatly by variations in borehole diameter. This effect could be minimized by locating a transmitter above and below the receiver string. By averaging the velocities obtained by the two transmitters, the majority of the borehole diameter effects would be eliminated.